11-1996

Experimental Validation of Finite Element Analysis Software Applied to the Design of a Motorcycle Swingarm

Bret Schaller
Embry-Riddle Aeronautical University - Daytona Beach

EMBRY-RIDDLE AERONAUTICAL UNIVERSITY

EXPERIMENTAL VALIDATION OF FINITE ELEMENT ANALYSIS SOFTWARE APPLIED TO THE DESIGN OF A MOTORCYCLE SWINGARM

A THESIS SUBMITTED TO

THE FACULTY OF THE OFFICE OF GRADUATE PROGRAMS

IN CANDIDACY FOR THE DEGREE OF MASTER OF AEROSPACE ENGINEERING

DEPARTMENT OF AEROSPACE ENGINEERING

BY

BRET SCHALLER

DAYTONA BEACH, FLORIDA

NOVEMBER, 1996

EXPERIMENTAL VALIDATION OF FINITE ELEMENT ANALYSIS SOFTWARE APPLIED TO THE DESIGN OF A MOTORCYCLE SWINGARM

by

Bret Schaller, B.S., E.I.T.

This thesis was prepared under the direction of the candidate's thesis committee chairman, Professor Charles Eastlake, M.S., P.E., Department of Aerospace Engineering, and has been approved by the members of his thesis committee. It was submitted to the Office of Graduate Programs and was accepted in partial fulfillment of the requirements for the degree of Master of Aerospace Engineering.

THESIS COMMITTEE:

Charles N. Eastlake

Charles Eastlake, P.E., M.S.

J. G. Ladesic

J. G. Ladesic, P.E., Ph.D.

Howard D. Curtis

Howard Curtis, P.E., Ph.D.

Department Chair, Aerospace Engineering

Dean of Faculty, Daytona Beach campus

12/10/96

Date

ACKNOWLEDGMENTS

The goal of personal achievement has been the driving force to complete my thesis. The love and support of my wife, Diane, has empowered me to achieve it.

I would like to thank my advisor, Professor Chuck Eastlake, for all the courses and special projects, for the advisement on this project, and most importantly for being an inspirational role model.

In addition, I wish to acknowledge as especially helpful the detailed reviews of various stages of the revised manuscript by Dr. J.G. Ladesic, P.E. and Dr. Howard Curtis, P.E.

ABSTRACT

Author: Bret Schaller

Title: Experimental Validation of Finite Element Analysis Software Applied to the Design of a Motorcycle Swingarm

Institution: Embry-Riddle Aeronautical University

Degree: Master of Aerospace Engineering

Year: 1996

This thesis documents the experimental validation of finite element analysis software applied to the design of a motorcycle swingarm. The process includes design and implementation of an onboard data acquisition system; definition and measurement of operational loads; laboratory correlation of loads; experimental validation of Pro/Mechanica finite element analysis software; design and prototype development of a single-sided motorcycle swingarm; and computer modeling using the Pro/Engineer solid modeling package.

Table of Contents

List of Tables

List of Figures

1. Background On Motorcycle Swingarm

The prevailing front wheel suspension design for motorcycles utilizes a spring and damper inside a telescopic fork. Rear wheel suspension is typically composed of a lever arm (swingarm), spring, and damper (Figure 1). The swingarm connects the rear axle to a pivoting mount on the vehicle. Rotation about the pivot point is governed by the spring and damper. Considering the complete system, the springs support the vehicle while the dampers restrict oscillation. Any mass not supported by the springs (wheels, brake calipers, swingarm, etc.) is defined as unsprung mass (Smith, 29).

As the vehicle passes over bumps and other surface irregularities, the suspension, working against the inertia of the unsprung mass, attempts to hold the wheels in contact with the road. Any reduction of the vehicle's unsprung mass greatly improves traction and handling. Consider traversing a bumpy corner. The cornering forces are transmitted to the pavement through the tires. If contact between the road and tires is not maintained, the vehicle will travel along a tangent to the curve instead of along the curve path. The forces attempting to separate the tire from the road are created by the reaction of the system's inertia to the surface irregularities. If the unsprung mass were zero, therefore zero inertia, the vehicle would have increased traction and corner better. The same methodology applies to braking over rough surfaces. With minimal unsprung mass, the tires have improved traction which is available for greater braking forces.

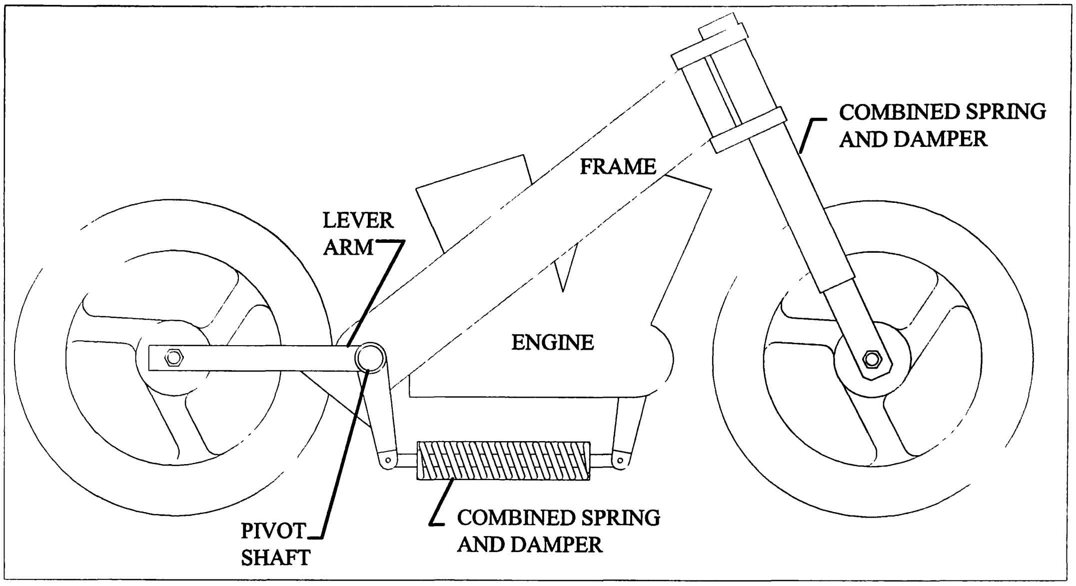

Figure 1. Sideview of Motorcycle

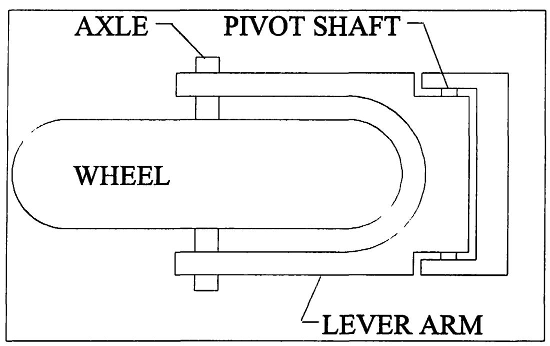

Figure 2. Top View of Swingarm Assembly

Motorcycle swingarms usually attach to the rear axle on both sides of the wheel. Through connections made by the axle and the pivot shaft, a closed loop structure around the rear wheel is created as shown in Figure 2. A single-sided design (Figure 3) is similar to an automobile wheel attachment. A stub axle is used to mount the wheel to the vehicle's suspension arm. This technique has been used sporadically on motorcycles as early as 1951 when Vespa used a stub axle to mount the front wheel on their ACMA model. More recently, single-sided rear suspension systems have become popular on race bikes such as the Ducati 916; Honda RC30, RC45, and Hawk; and the Bimota Tesi.

The major difference between the automotive and motorcycle applications is the amount of supporting structure available to transmit the wheel loads into the vehicle chassis. Side loads are a prominent contributor in automotive wheels. The ability to lean into turns on motorcycles redirects a large percentage of the side load into a vertical load. Regardless of the load scenario, the lever arm suspension design like that shown in Figure 2 does not lend itself to the use of stub axles. The vertical loads carried by motorcycles during turns are carried by the lever arms torsionally. This torsional force, if not fully constrained, pushes the front and rear wheel out of the same plane of rotation causing handling problems (Figure 3).

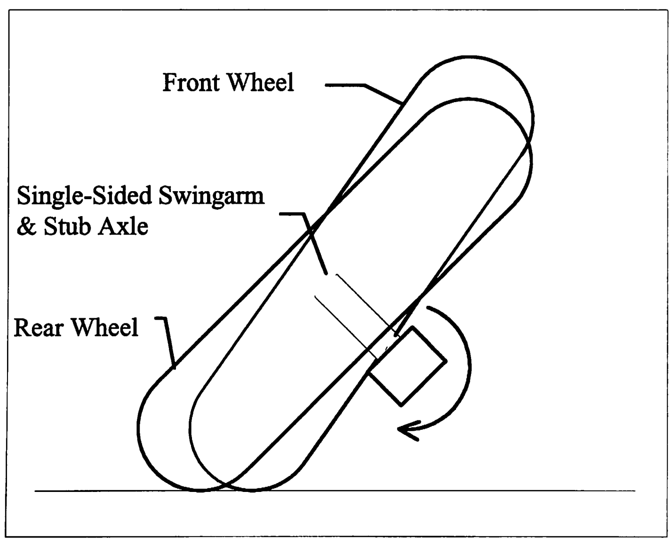

Figure 3. Rear View, Motorcycle Wheels

In spite of the additional torsional load encountered on single-sided suspension systems for motorcycles, the benefits of a sound design can be tremendous in racing applications. In endurance racing where pit stop time can win a race, tire changes on single-sided suspension bikes can provide the competitive edge required for a win. In addition, there is the potential to reduce the unsprung weight of the vehicle. Production vehicles can benefit from a single-sided design through unsprung weight savings, assembly time, and marketability. Whether the weight reduction greatly enhances the vehicle's handling is not as significant as is the demonstration of the technology the single-sided design provides. Market research has shown that the sport bike consumer values the technological aspect of the motorcycles as well as the performance (Miller).

2. Project Overview

The design of a new swingarm requires an understanding of the loading scenario encountered during operation. This was accomplished through a number of activities. The current production swingarm was fitted with strain gages. Data was then collected while the vehicle was being ridden. Recreating these strains using a hydraulic actuator applied to a fixtured swingarm developed the correlation between axle load and strain. The actual loads could then be deduced. This information was previously unknown.

In order to improve the accuracy of the finite element analysis software validation, a second experiment was constructed which omitted the components of the real swingarm configuration that could not be modeled accurately. These are the axle blocks that slide in the ends of the swingarm for drive belt adjustment, the tire/wheel combination, and the bearing load transfer through the axle into the swingarm. A detailed explanation of these variances from the actual assembly is in Sections 5.1 and 5.2.

The simplified part was then modeled using Parametric Technology Corporation's (PTC) Pro/Mechanica stress analysis software. A three dimensional representation of the swingarm with zero material thickness was generated. The various material thicknesses used throughout the part were assigned to the elements prior to running the analysis.

Utilizing the experimentally determined loads and corresponding strains coupled with the computer stress analysis model, experimental validation of the software was performed. The preliminary design of the single-sided swingarm was then initiated with the modeling methods developed from the preceding work.

3. Strain Measurement During Operation

3.1 Purpose

The operational loads of the swingarm are a function of the vehicle weight and the shock absorber spring. The motorcycle rides on the spring on the rear shock absorber and the springs inside the front fork tubes. The force required to compress the rear spring is directly proportional to the force induced into the swingarm assembly. The magnitude is dependent upon the suspension linkage. Referring to Figure 1, the portion of the swingarm connecting the axle to the pivot shaft is approximately twice the length of the member connecting the pivot shaft to the shock absorber. This produces a 2:1 ratio between axle motion and shock length.

The damping system imposes additional loading effects that are usually less than the maximum spring force. When the compression damping is maximized, traversing over sharp road irregularities can impact the system faster than the damping fluid can escape the internal chamber. This will act as an hydraulic lock on the shock and transmit the road impact through the swingarm and into the chassis.

The other possibility of exceeding the maximum spring force occurs when the suspension reaches the end of its travel. Suspension travel is limited to avoid contact and subsequent damage to parts like the rear fender, tailsection, and tail light. Safety is also a concern. With a maximum vehicle speed of 130 mph, unrestricted wheel movement could place the tire surface moving at 260 mph against the bottom of the rider's seat. The force to fully compress the suspension is calculated by multiplying the spring rate with the maximum allowable travel. The force applied in addition to the full compression load must be measured. This additional force is only encountered when a severe bump, hole or some form of road debris is traversed. Road conditions being random required that some judgment be made as to the worst case obstacle. Strain data taken on the swingarm was used to interpolate the magnitude of the force applied to the tire.

3.2 Define Existing Part

Figure 4 illustrates the current double-sided swingarm, Swingarm 1. The various components of the welded swingarm assembly are labeled. Table 1 provides the corresponding material thicknesses.

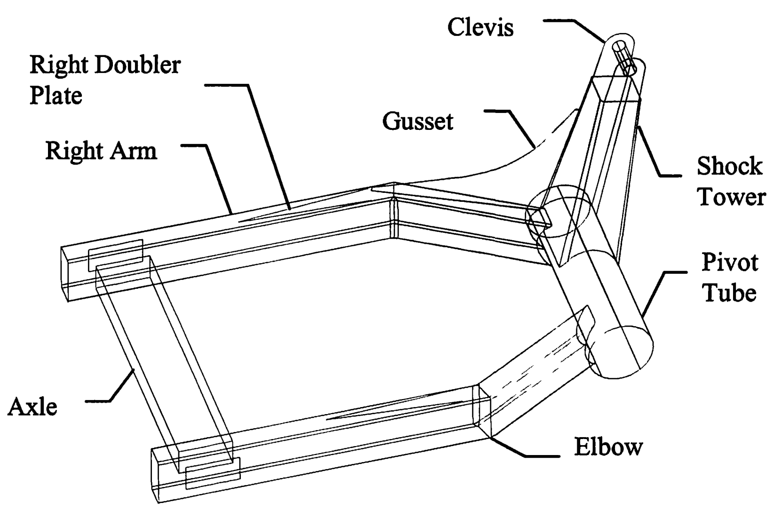

Figure 4. Double-Sided Swingarm (shown upside down)

Part Name	Material Thickness
Shock Tower	13 gage (.0897 in.)
Pivot Tube	ID 2.125 in., OD 2.380 in.
Doubler Plates	.083 in.
Arms	1x2x.083 in. wall
Axle	1x2x.083 in. wall
Gusset	12 gage (.1046 in.)
Clevis	7 gage (.1793 in.)

Table 1. Swingarm Material Thicknesses

3.3 High Stress Area Identification

Stress Coat, a brittle painted-on material that cracks when the surface to which it is applied deflects, was used to identify the areas of concentrated stress. By coating then loading a calibration bar along with the test specimen, the spacing between the cracks can be correlated to actual strain values. For this project, the Stress Coat was used only to identify the location and direction (maximum strain occurs perpendicular to crack direction) for various strain gages. The cracks are similar to contour lines or fringe plots. While these fringe plots are of undetermined magnitude, they accurately define the stress concentration areas and corresponding directions for each type of strain gage. This initial step could have been performed analytically by applying estimated loads to the Pro/Mechanica model and performing the analysis; but the validity of calculated results for this structural shape is unproven and is, in fact, part of the objective of this thesis.

3.4 Swingarm Strain Gages

Unidirectional and torsional gages were chosen based on the particular location where they were to be installed on the swingarm. The intent was to investigate areas that would provide strains of high magnitude. This would provide good strain sensitivity for the instrumentation system. Three unidirectional gages, U1, U3, and U4, were used on the bottom surface of the arms at the elbows as shown in Figure 5. Two unidirectional gages, U6 and U7, were used on the shock tower. The torsional gages, T1 and T2, were applied midway along the longest section of the arms in the middle of the two inch surface. An additional torsion gage, T3, was used on the pivot tube. Two more uniaxial gages, U2 and U5 respectively, were applied on the inside surface of the left elbow and at the interface of the left arm and the pivot tube.

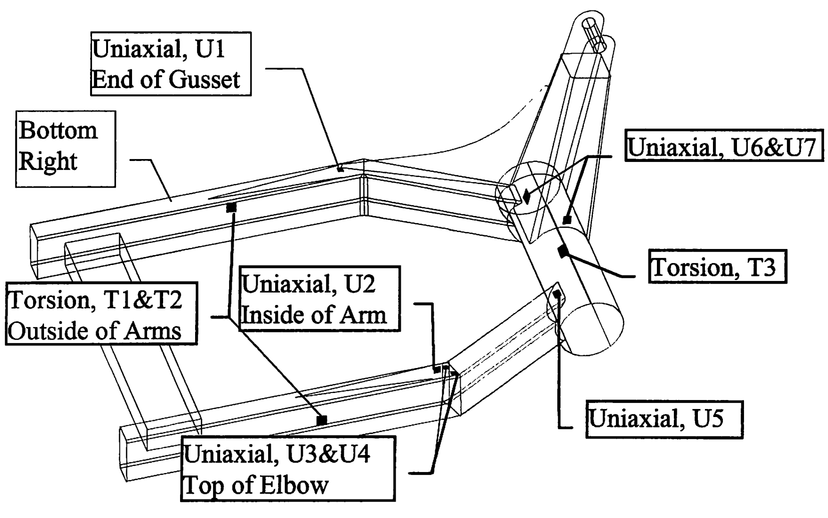

Figure 5. Strain Gage Locations, Swingarm 1

Measurements Group, Inc. gages were used. The CEA-06-062UW-350 uniaxial type and the CEA-06-187UV-350 torsion gages were chosen for size, coefficient of thermal expansion, and resistance value of 350 ohms. These are suitable for a 10 volt excitation voltage. Using the 10 volt bridge over a 5 or 3 volt configuration provides a larger magnitude signal. Thermal gradients induced in small gages or stacked rosettes due to gage heating are the main disadvantages of a 10 volt system. The uniaxial gages were sufficiently large to avoid any heating problems.

3.5 On Board Data Acquisition System

A 1995 Buell S2 Thunderbolt was used to generate the service load data (Figure 10). It was determined that the type of maneuvers which generate the maximum service loads would require an on board data acquisition system (DAS). The strain gaged swingarm was installed as was the on board DAS. Since maneuvers may fall outside the constraints of the traffic law, a closed course not using public roads was used. The infield, back straight-away, and the Harley-Davidson Bump Course all located inside the Talladega Speedway in Lincoln, Alabama were selected.

3.5.1 Instrumentation Selection

Researching portable data acquisition systems identified a number of units acceptable for such automotive work. The size constraints dictated by a sportbike considerably limited the selection. The choices were IO Tech's Daqbook 200 in conjunction with a laptop computer (Figure 6), the Somat system (Figure 7), and building the system up from the circuit board level (Figure 8).

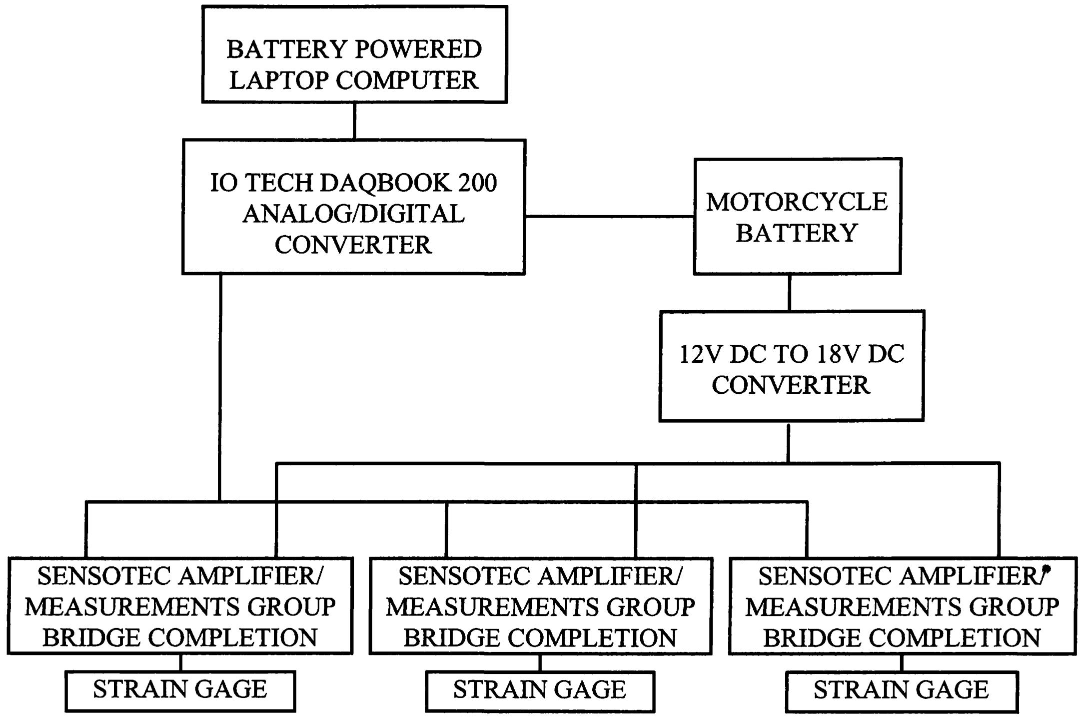

Figure 6. IO Tech Daqbook 200 / Laptop Computer System

The IO Tech Daqbook 200 is a boxed analog to digital converter. Data is transmitted to a PC via the parallel port. The advantage of the boxed A/D card and parallel port transfer is that a laptop computer can be used. This allows large amounts of memory and disk space in a relatively inexpensive system. An additional advantage of this system is the transfer rate of the parallel port. Data is streamed directly to the hard drive. All of the other systems require data streaming to RAM. Although this is fast and functional, for large volumes of data it is expensive. The Daqbook 200 sells for $2000, and the laptop can be purchased for as little as $1000. The Daqbook 200 connected to a 486DX laptop computer was used for this project.

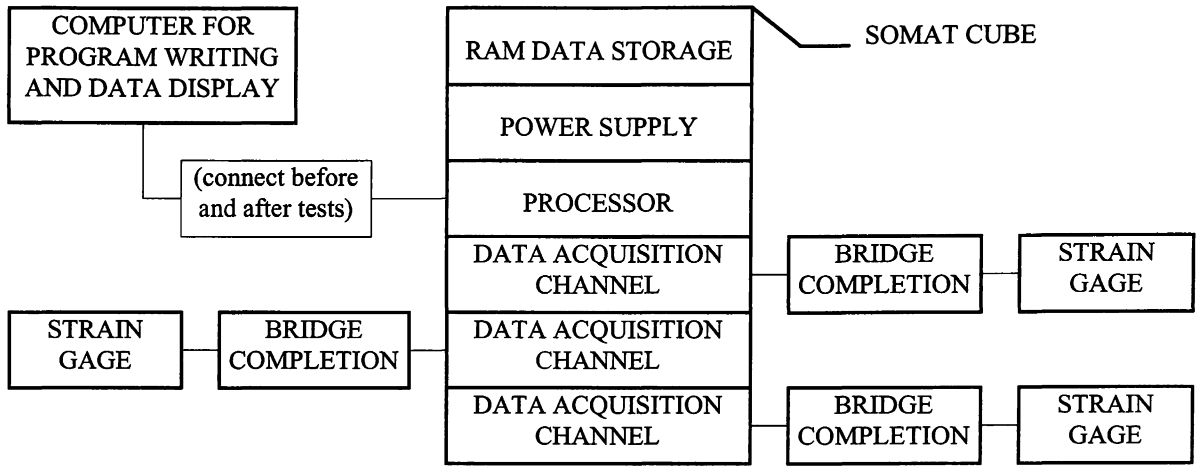

Figure 7. Somat System

The Somat system is a self-contained data logger. It has the capacity to perform real time frequency analysis and produce waterfall plots. It is still classified as a data logger due to its inability to display the data. The unit must be plugged into a PC to upload data acquisition programs and download data. The cost of a Somat system starts at $5000 for one channel and approximately $1000 for each additional channel. With four channels for this portion of the project, the laptop, and the Somat cube, the total cost is approximately $9000 for this system. The size and durability of the Somat system is the best of all three investigated. The storage capacity is limited to the number of RAM modules purchased. At $2000 per megabyte of RAM, the overall cost of this system ruled it out for this project.

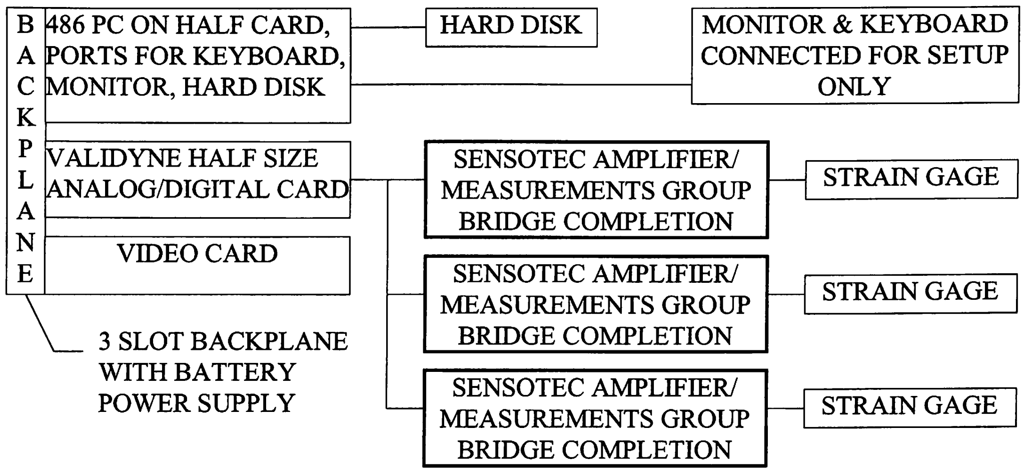

Figure 8. Á La Carte System

All of the components are available for building a portable DAS á la carte. Three slot backplanes complete with an enclosure large enough for half-size PC cards are available with power supplies and ports for peripherals. Validyne has a half size A/D card with acceptable speed for strain gage work. There are 386 and 486 PC's on half cards. These come complete with plugs for keyboard, monitor, printer, mouse, hard drive, etc. The third slot is used for a video card. Data can be stored on flash RAM through a PCMCIA/hard disk connection or directly on a hard disk. Starting and stopping the data collection sequence can be done using a trigger mechanism, such as a known voltage applied with a switch. This technique is usually done using one of the available channels. A power supply, such as a nine volt battery, is switched across one of the available data channels. The software monitors this channel and executes the data acquisition sequence when the voltage signal is applied or removed. An alternate solution is to set up the run with the keyboard and monitor plugged in, then unplug them without turning the system off. A smaller keypad can than be plugged in and used to trigger the data acquisition sequence.

The components of this system totaled approximately $3000 for materials only. It was estimated that an additional 40-50 hours of labor would be required for assembly, trouble shooting, and setup. Without a monitor or indicator lights, the major concern was not knowing whether the data collection sequences were triggered properly. This could be resolved with additional hardware. This system was not pursued due to the uncertainty of this issue and the troubleshooting problems usually encountered when setting up new systems.

All of these systems require software to connect the A/D data acquisition cards to the computer processors and the data storage disks. The Somat system requires a $2000 proprietary package. The other two systems come with a minimal source code software package. With some computer programming experience, these packages could be modified to be useful for data acquisition in a variety of experiments. There are a number of Microsoft Windows based programs available in the $1500 to $2000 range. The HEM Datasys' Snap Master data acquisition software was used.

3.5.2 Signal Conditioning & Calibration

Due to the relatively small differential voltage produced by the resistance change of the strain gage, amplification is needed for accurate measurements. A Wheatstone bridge was also used to increase the sensitivity. This signal conditioning was performed using an In-Line Amplifier from Sensotec equipped with MR1-350-130 bridge completion pads from Measurements Group. Strain gages were wired directly to the MR1-350-130 pads inside the Sensotec boxes. The amplified signal was then wired into the Daqbook.

Prior to data collection, potentiometers inside the Sensotec boxes were used to zero the signal. Shunt resistors were placed in parallel with the strain gages to produce voltage signals equivalent to a known microstrain. This calibration factor was entered into the data acquisition program and used as the data was recorded.

HEM Datasys Corp. Snap Master software was used. A hardware specific driver for the Daqbook 200 was bundled with the software. This provided a drag and drop method of setting up the data acquisition instrument. Once the Sensor, IO Tech A/D, Display, and File Save elements were placed on the screen and linked, the software handled all of the internal instructions to and from the parallel port, video display, and hard disc (Figure 9).

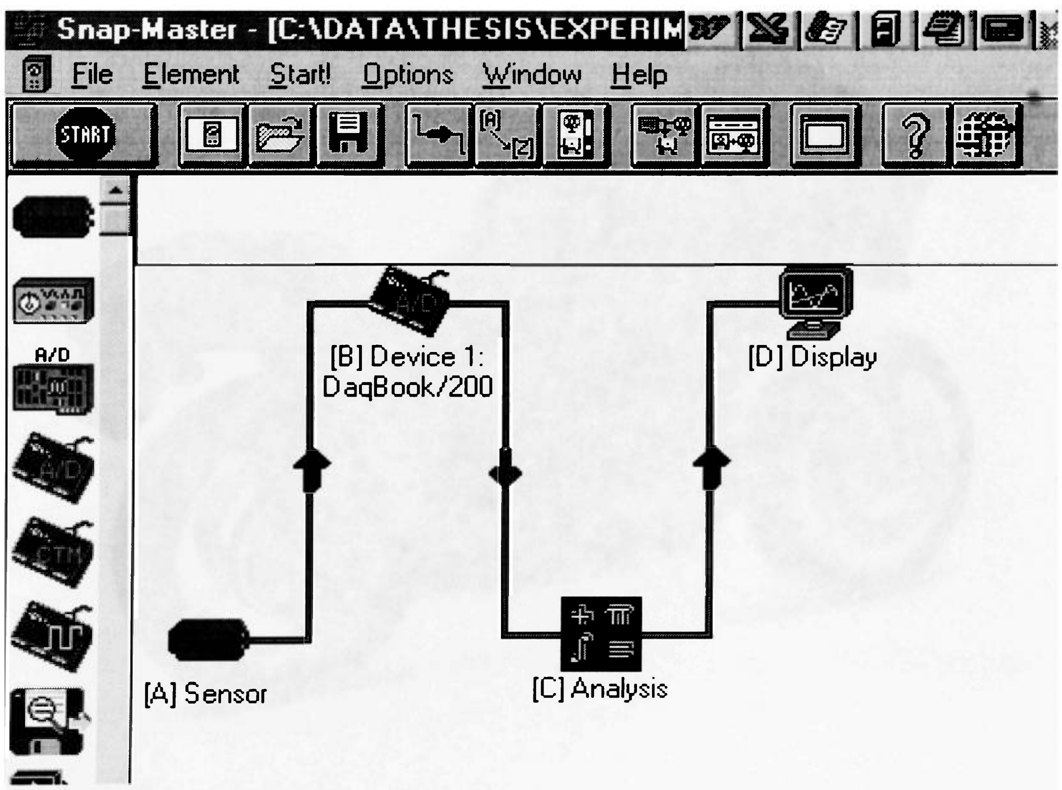

Figure 9. Data Collection Instrument Display

3.6 Data Collection

Data was recorded as the test rider executed a variety of maneuvers while riding a 1995 Buell S2 Thunderbolt (Figure 10). Only data required to define the operational envelope was required. Resource constraints when the data was collected prevented taking photos for the actual test bike performing the maneuvers. The following photos are provided to assist in defining the maneuvers:

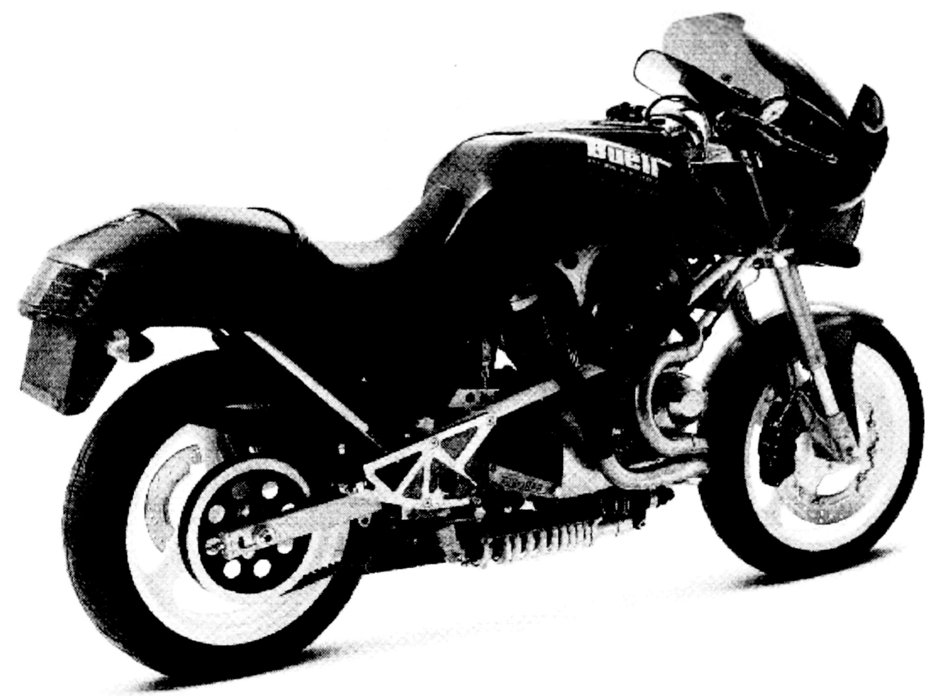

Figure 10. Buell S2 Thunderbolt (Buell)

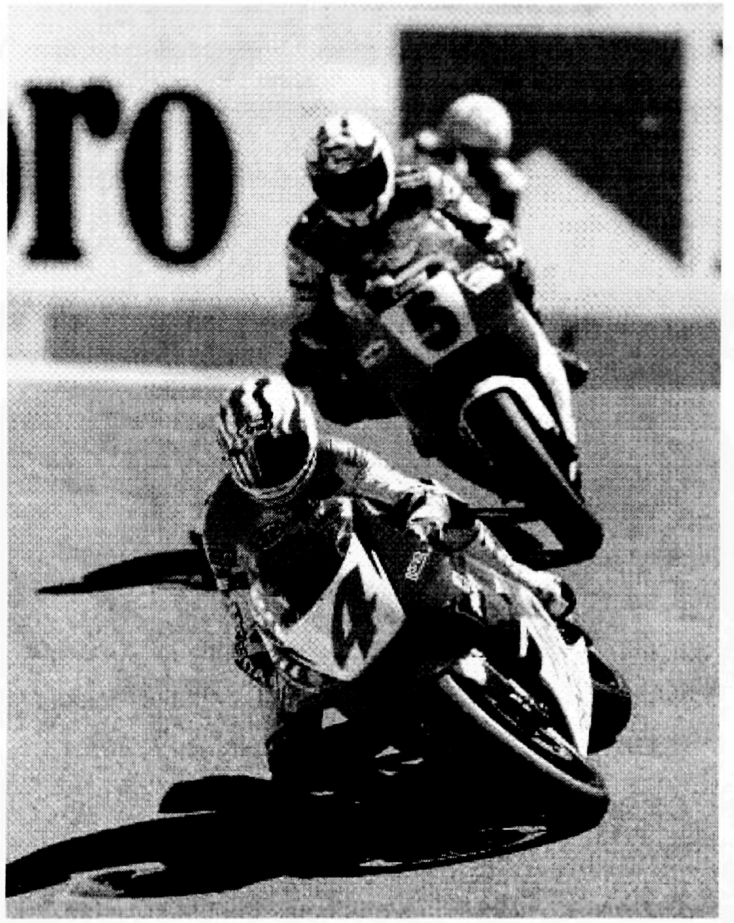

Figure 11. Slalom Maneuver
'Corkscrew' photo courtesy of Brian J. Nelson (Motorcycle)

The "slalom" maneuver consists of transitioning the motorcycle from full lean on one side to full lean angle on the other side. (Figure 11)

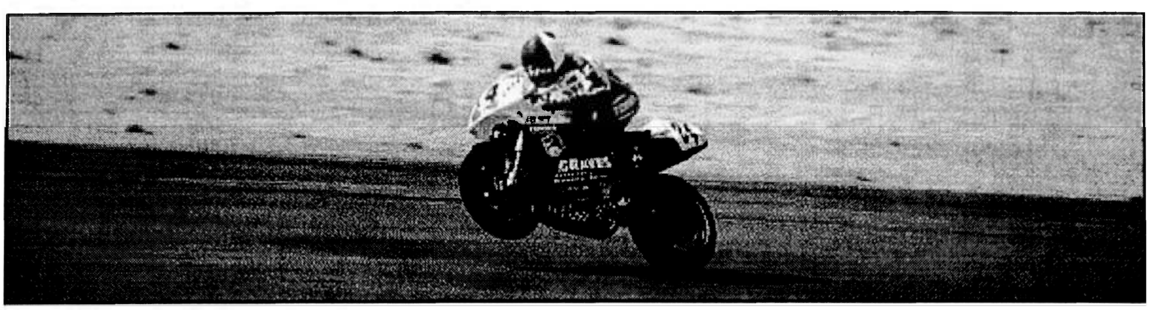

Figure 12. Wheelie Maneuver (Motorcycle)

The "wheelie" maneuver consists of raising the front wheel off the ground by rotating the entire motorcycle about the axis of the rear wheel. Figure 12 illustrates this maneuver on a Buell S1 Lightning at the Streets of Willow race track.

Figure 13. Stoppie Maneuver

Photo courtesy of Tom Fortune (Honda)

The "stoppie" maneuver consists of aggressively decelerating the motorcycle using the front brake only. As the vehicle weight transfers to the front wheel, the rider adjusts his/her position above and forward of the vehicle's center of gravity until the rear wheel lifts off the ground (Figure 13). The force required to lift the rear wheel is maximum when the motorcycle is level. This circumstance requires that the rider immediately readjust his position once the rear wheel lifts. This maneuver is important to rear suspension arm design because it introduces some of the highest loads into the system.

The slalom maneuvers produced the highest torsional data recorded. These strains, while being the largest torsional readings, were all under 500×10^{-6} in./in. ($500\mu\varepsilon$). This compliments the design of the swingarm by indicating that minimal deflection occurs when cornering. Chassis deflection during cornering is analogous to compressing a spring. When the compressive force is released, the spring snaps back and oscillates until it damps out. This dynamic behavior is detrimental to stability.

The wheelie and stoppie data were comparable, with the stoppie values being larger. Wheelies produced a strain increase when the rear of the vehicle squatted as the clutch engaged the transmission to the engine generating the torque to raise the front wheel. The stoppie generated a short duration, high magnitude strain reading when the rear wheel recontacted the ground. The magnitude is related to how high the test rider raises the rear wheel during the maneuver.

The intent of the test plan was to record data during the worst case loading scenario that a customer could expect to encounter. The cyclic load required for fatigue calculations is generated from the vehicle load on the rear wheel and the shock spring rate. While the stoppies produced the highest strains, they were dependent on the height of the stoppie and the method in which the rider landed. If the rider was standing on the footrests, sitting on the seat, or distributed between the two when the rear wheel hit the ground, the weight distribution over the front and rear wheels was significantly affected.

By placing the rider and vehicle weight completely on the rear wheel in a wheelie maneuver, the maximum possible rear wheel load could be simulated. With an Emergency Medical Technician on hand, the test rider wearing a significant amount of safety equipment rode the test vehicle, balanced on the rear wheel, across an 18 inch wide, 4 inch deep hole. The vehicle was not statically balanced on the rear wheel with the center of gravity of the system being directly above the contact patch of the tire. It was balanced by the torque of the engine and the weight of the vehicle such that the attitude of the vehicle was close to horizontal. Fortunately, there were no problems with the data collection. This wheelie maneuver produced the 3000με reading on gage U3 (Figure 5). For reference, gages U3 and U4 are located on either side of rosette R1 (Figure 19). Only this microstrain value was used in the following section to determine the rear wheel load in pounds.

3.7 Error Check

The strain gage data are collected to determine the accuracy of the Pro/Mechanica finite element package. To insure the accuracy of this data a number of standard techniques were employed. The following three were recommended by Darryl Peterson, Application Engineer for Measurements Group, the manufacturer of the strain gages used for this project:

1. Optical Inspection
2. Zero Return
3. Holding Load Constant

The optical inspection checks for visible damage to the gage and lead wire connections. The zero return verifies that the gage reading returns to the initial value after the load has been released. Checking that a constant load produces a constant reading verifies that transient signals (thermal, electrical, magnetic) are not present.

In addition to the checks recommended by the manufacturer, Peter Stein suggested the following technique in a seminar on measurements. A check gage was used for the onboard data collection. This is basically a non-stressed strain gage placed near the gages being measured. Any change in signal on this gage during the test would indicate the presence of an external signal superimposed on the collected data. This technique is useful on the motorcycle due to potential anomalies induced by the vehicle's charging system or present at the test track.

As mentioned previously, the rosettes were checked for thermal transients. Small, stacked rosettes are susceptible to heating effects. Both rosettes were powered with the 10 volt excitation for fifteen minutes. There were no changes in the output signal.

The remaining link in the strain collection sequence was the load cell. The calibration certificate provided with the load cell was verified using known loads.

4. Laboratory Correlation of Service Loads

4.1 Test Fixture & Equipment

Swingarm loads generated while riding the vehicle were identified in a laboratory. The same gaged swingarm used for the vehicle tests was mounted in a test fixture. Loads were applied to a simulated wheel hub until the strain values recorded during the road test were recreated (Figure 14).

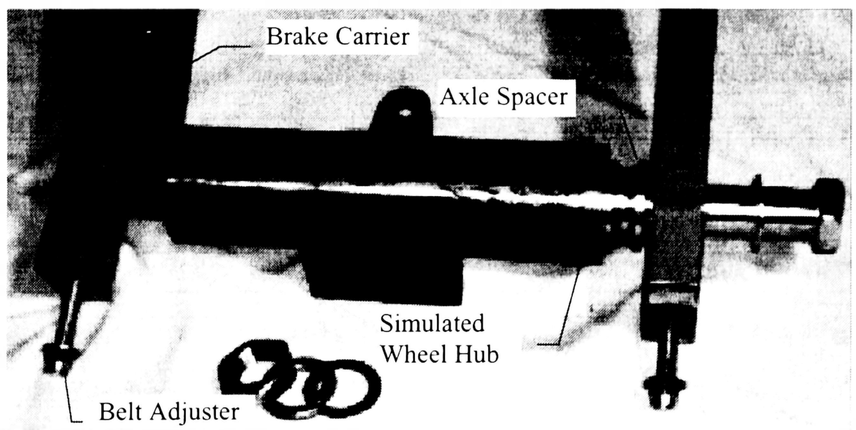

Figure 14. Laboratory Axle Assembly

With the exception of the wheel hub and shock absorber, the fixture was composed completely of the production components to which the swingarm mounts. In place of the shock absorber, a rigid member was used. A long member was used instead of just pinning the swingarm clevis to assure that the force provided by the member was in the same direction as the force developed by the shock absorber.

The load received by the swingarm through the tire and rim was applied to the steel cylinder (simulated wheel hub) shown in Figure 14. This cylinder was made to the same dimensions as the hub and fitted with bearings.

Using this hub along with production parts for the spacer, rear brake carrier, wheel bearing spacer, and wheel bearings, the axle was assembled and torqued to the specified 70 ft-lbs. A hydraulic actuator applied the load at the center of the hub. Applying the load through a gimbal avoided imposing a constraint against rotation that does not exist in the actual assembly.

4.2 Static & Dynamic Load Equivalents To The Service Load

A load cell was used in series with the hydraulic ram. The three gages comprising the rosette R1 were wired into the data acquisition system and programmed to display principal strain. R1 was chosen because it provided the largest strain reading throughout the test. The MTS controller applied an increasing load to the hub until the rosette measured 3000$\mu\varepsilon$ on gage U3. This occurred under a static load of 1450 lbs. and a 3 Hz sinusoidal dynamic load of 1293 lbs. The static load was determined for the stress analysis software validation. The dynamic load was identified for use in the single-sided swingarm design. The 3 Hz frequency was chosen simply because the hydraulic actuator and pump used were capable of producing the 1293 lbs. force at this rate over the deflection distance inherent in the system.

Note that 3000$\mu\varepsilon$ is equivalent to 90,000 psi which is above the minimum yield strength of 75,000 psi for 4130N chrome moly steel (MIL-T-6736B). This demonstrates that it is possible to induce local yielding on this part during extreme conditions. Because this maneuver was only used to define the maximum service load possible, the excursion outside the linear portion of the stress strain curve was deemed acceptable. Additionally, the published value of 75,000 psi yield strength is a statistical value indicating the lowest possible value. Samples were tested from two different swingarms with resulting yield strengths of 100,000 psi and 97,500 psi. (Technimet).

5. Experimental Data Collection

The original swingarm, Swingarm 1, used in Chapter 3 was destroyed during destructive fatigue testing following the measurements that were needed for this project. Better planning would have stayed the destructive testing until this project was completed. A second swingarm, Swingarm 2, which was a nominally identical production part was used for this stage of data collection. As pointed out previously, the Swingarm 1 strain gage locations were chosen based on the Stress Coat results. The goal was to capture the highest levels of strain for each location. The Swingarm 2 gage locations were chosen to test the analysis software. The gages were located where strain gradients were large, the geometry was concentrated, or where the strains could be found by hand calculation.

The complete swingarm assembly on the vehicle has numerous transfer points along the load path from the ground to the rear shock absorber. These begin with ground contact through the tire to the rim. The rim transfers vertical and longitudinal loads via bearings to the axle. The wheel bearings eliminate the possibility of a moment about the axle. Torsional loads, however, can be generated by side loads into the tire during cornering. These are transmitted from the hub, through the brake carrier and spacer (Figure 14), and into the swingarm due to the clamp load of the axle. Axle slider blocks are used inside the hollow section of the 1x2 box tubing of the swingarm (Figure 15).

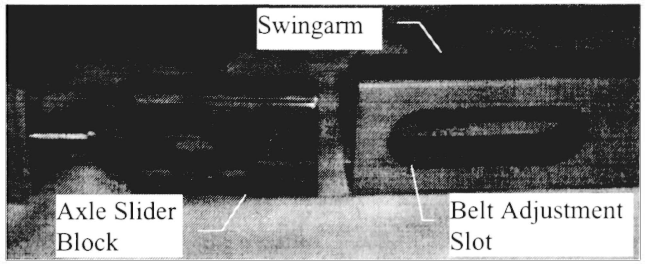

Figure 15. Axle Slider Block

These carry the compressive load of the axle torque through the swingarm, and allow belt adjustment by sliding fore and aft before axle torque is applied. These various methods of load transfer are difficult to model accurately. To remove some potential sources of error, a revised assembly was used. In place of the tire, rim, axle, bearings, and axle slider blocks, a 1x2 piece of chrome moly tubing was used. This allowed the tire load to be transferred directly into the belt adjustment slots on the swingarm (Figure 16).

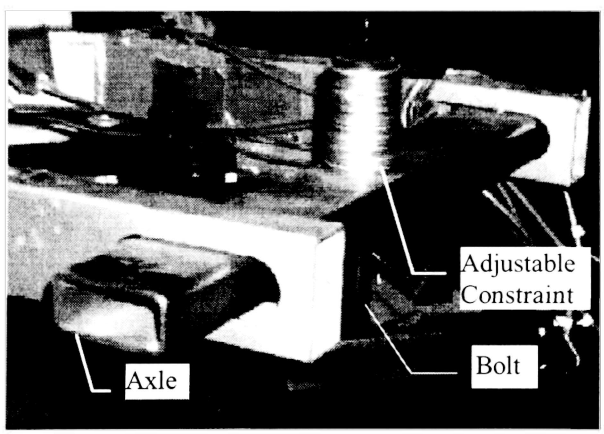

Figure 16. Axle Constraint

5.1 Loads & Constraints Selection

Once the maximum service load was established at 1450 lbs., a range of loads was chosen at 200 lb. increments for loads of 600 - 1400 lbs. This produced a sufficient range for comparison and allowed a linearity check as well. Correcting for the moment arm lengths on the swingarm, the equivalent loads were applied at the shock absorber clevis while the axle was constrained as shown in Figure 16. Using the standard 12mm shock absorber fastener, the clevis held the eyebolt on one end of the load cell (Figure 18).

The swingarm mount block, an aluminum casting that connects the swingarm to the engine case, was clamped to the test bench. With the exception of a 90 degree rotation on the orientation of the swingarm mount block to the swingarm, the swingarm pivot was assembled exactly as on the production assembly. This includes all of the production components and assembly processes.

As described above and displayed in Figure 16, the axle and related components were replaced by a 1x2x.083 in. wall tube. The effective area the load was transferred through switched from eight semi-circular sections to four rectangular ones (Figure 17).

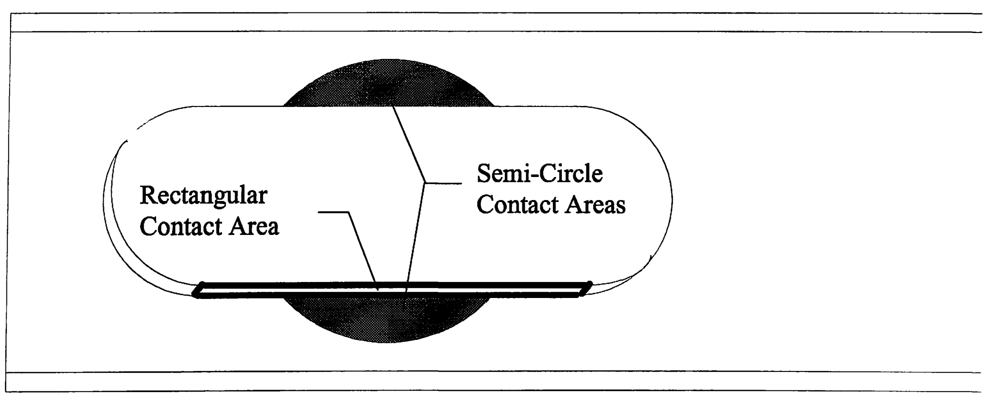

Figure 17. Axle Load Transfer Points

Additionally, the original method applied the load in shear above and below the axle through the semi-circle contact areas shown in Figure 17. The revised setup applies the load in compression above the axle only in the rectangular contact area. In the immediate area surrounding these constraint points, these variances will have a significant effect on the strain.

Since this area is inherently overdesigned due to the manufacturing processes of tubing (i.e. a tapered cross-sectional area matches the stress distribution along an end-loaded beam in bending closer than a constant area), this variance in constraints is believed to be an acceptable substitution. The production components were used when defining the load that correlates to the maximum strain recorded while riding the motorcycle. Now that the maximum load has been identified, these changes to the various components to facilitate the computation model are possible.

The actual load was applied as a constraint. While the shock absorber clevis was receiving the load from the hydraulic ram, a bolt was constraining the axle from motion as shown in Figure 16.

5.2 Test Fixture & Equipment

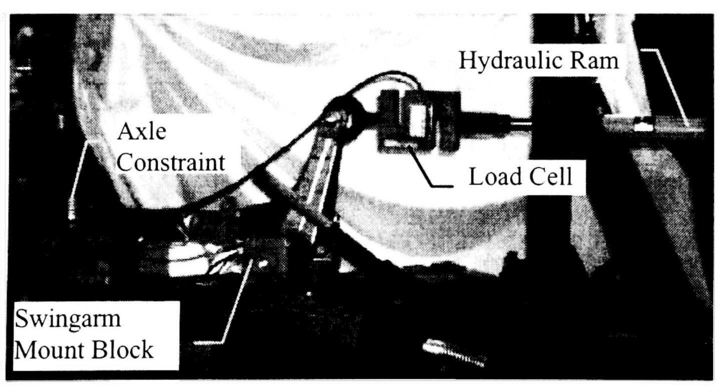

Figure 18. Laboratory Setup

The entire test assembly was clamped to a 'T' slotted surface plate similar to the bed on a milling machine. The hydraulic ram was held horizontal with a reinforced upright. The load cell was fitted between the ram and the swingarm pivot clevis. The swingarm pivot was held to the surface plate via the swingarm mount block (Figure 18). A threaded adjuster attached to the axle band was used to set the swingarm horizontal and aligned with the hydraulic ram shaft (Figure 16).

The onboard data acquisition system was also used for this laboratory setup. The only difference is a 120 volt input / 18 volt output power supply was used to power the Sensotec boxes with the required 18 volts, instead of using the batteries employed in the road test.

5.3 Gage Selection & Placement

Along with four uniaxial gages of the type described in section 3.4, two WK-06-060WR-350 rosette gages were also used in the laboratory data collection phase. Rosettes were added to provide principal strains for comparison to the theoretical analysis. It was necessary to include principal strains in the data set. These gages would not be sensitive to misalignment errors between placement on the part and measurements read along various axes from the screen. Due to the potential for thermal errors from using a 10 volt excitation signal with stacked rosettes, a zero signal was monitored for fifteen minutes. The signal remained constant. Figures 19-23 illustrate the gage locations.

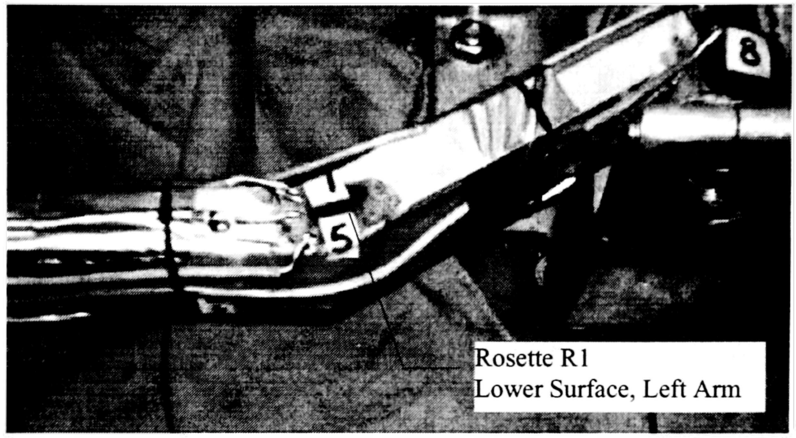

Figure 19. Rosette R1 (Gages 5,6,7)

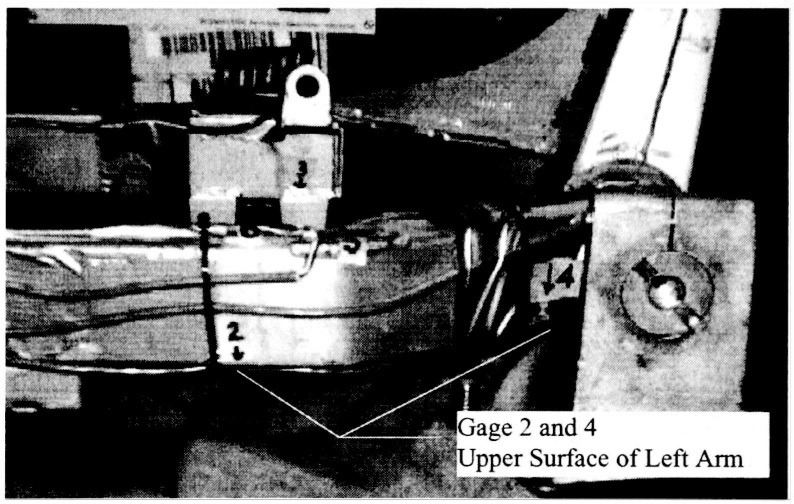

Figure 20. Gages 2 and 4

Gage 2 is mounted opposite Rosette R1 when viewed using a horizontal mirror plane. Gage 3 is mounted opposite Gage 2 when viewed using a vertical mirror plane. Gage 4 is located just outside the weld area where the arm attaches to the pivot tube.

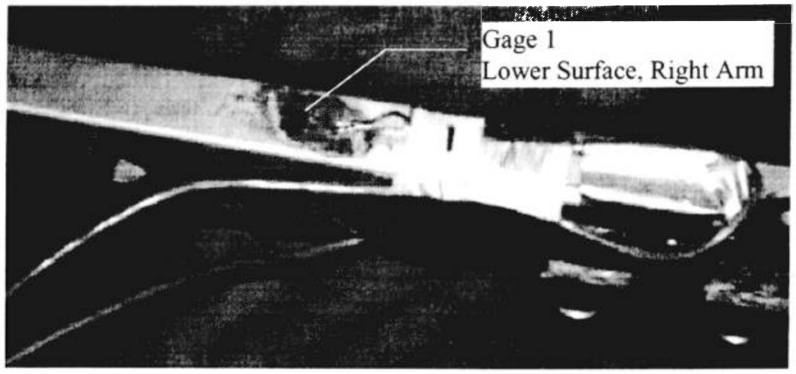

Figure 21. Gage 1

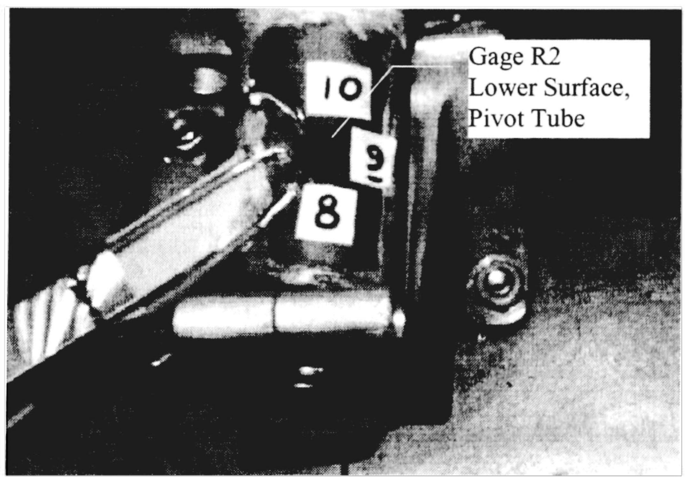

Figure 22. Rosette R2 (Gages 8,9,10)

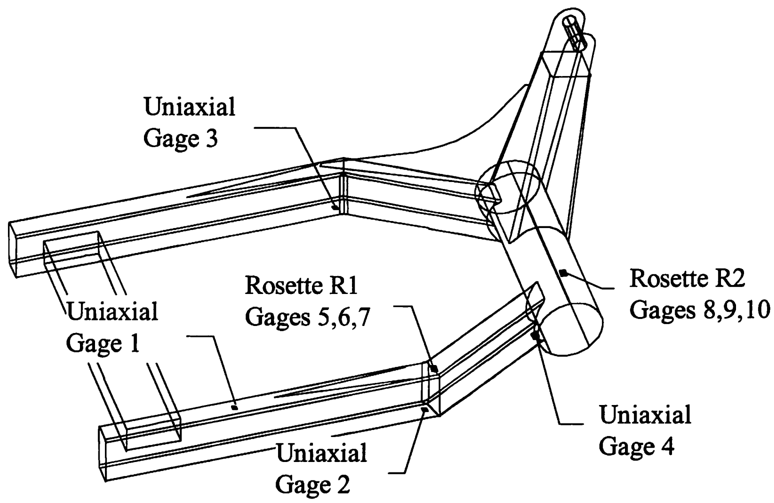

Figure 23. Strain Gage Location, Swingarm 2

5.4 Data Collection & Reduction

The equipment was capable of recording up to 16 channels. With three gages per rosette, four additional uniaxial gages, and the load cell, there were eleven channels total. Wheatstone bridge completion and amplification was available for only six channels. The data was taken in two runs recording one rosette and two single gages along with the load cell during each run. With real time display on the computer monitor, all six channels recorded data at 50 Hz as the hydraulic ram was hand pumped to the 3000 lb. mark. The sample rate was chosen to collect a sufficient number of points during the timespan required to hand pump the ram. A 3000 lb. maximum load was applied at the tower to insure the data set encompassed the load equivalent to 1400 lb. applied at the axle. Figure 24 displays the raw data recorded for five strain gages and the load cell during one test run.

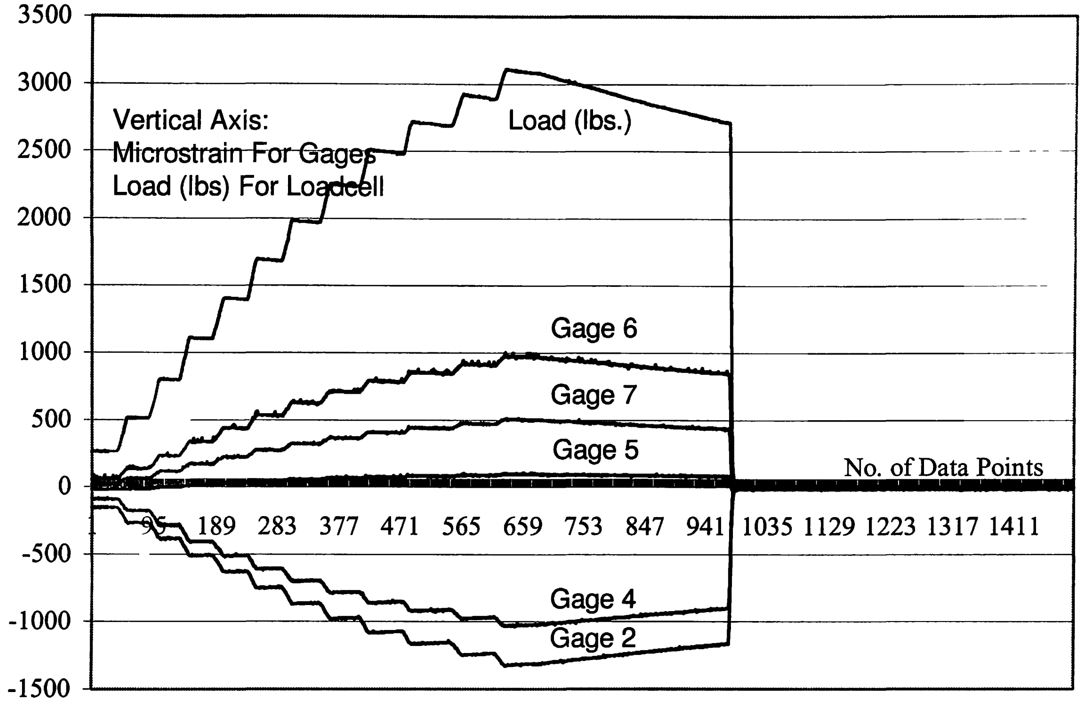

Figure 24. Raw Data, Microstrain And Axle Load vs Data Point

Although shielded wire and connections were used, there was always some amount of 'noise' in the system. A smoothing filter was used to reduce this environmental and electronic noise. Figure 25 displays the same data in its raw and smoothed format.

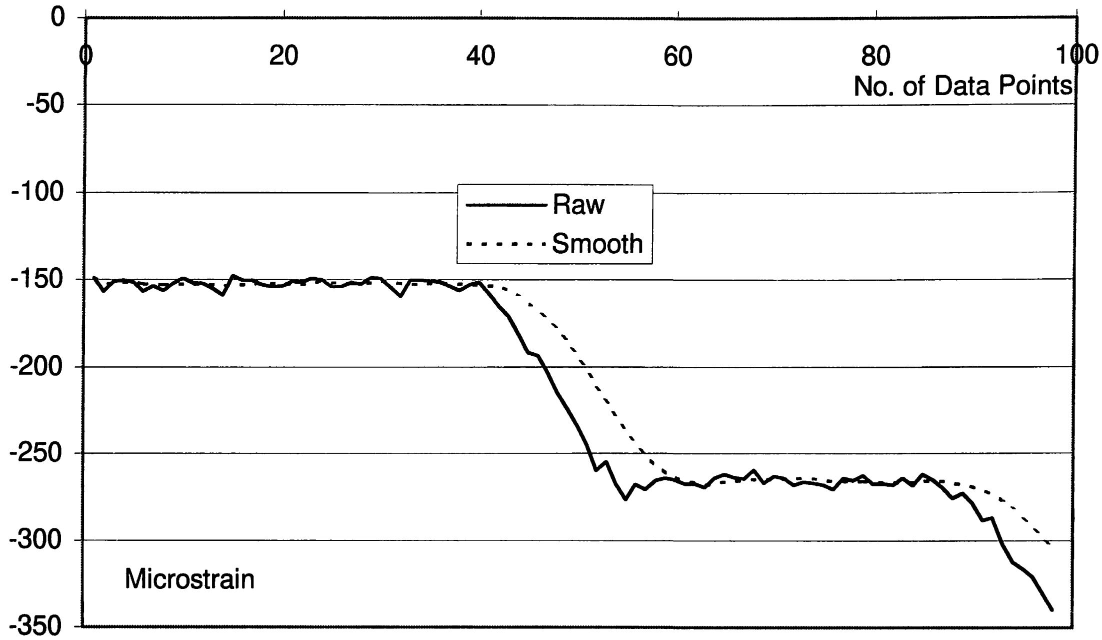

Figure 25. Smoothed And Raw Data, Gage 2

For steel and many other materials, load versus strain within the yield limits for the specific material is a linear relationship. Figure 26 displays smoothed data and linearized data for the same channel. It is believed that slight non-linearity of the data is attributable to experimental error. By linearizing it using the least squares method, some of this error is removed. However, it is possible that the swingarm assembly, composed of multiple stampings, tubing, and stitch welds produces a slightly non-linear load versus strain curve. This could be attributed to the induced stresses created during the welding and stamping processes, or simply to the unsymmetric shape of the structure.

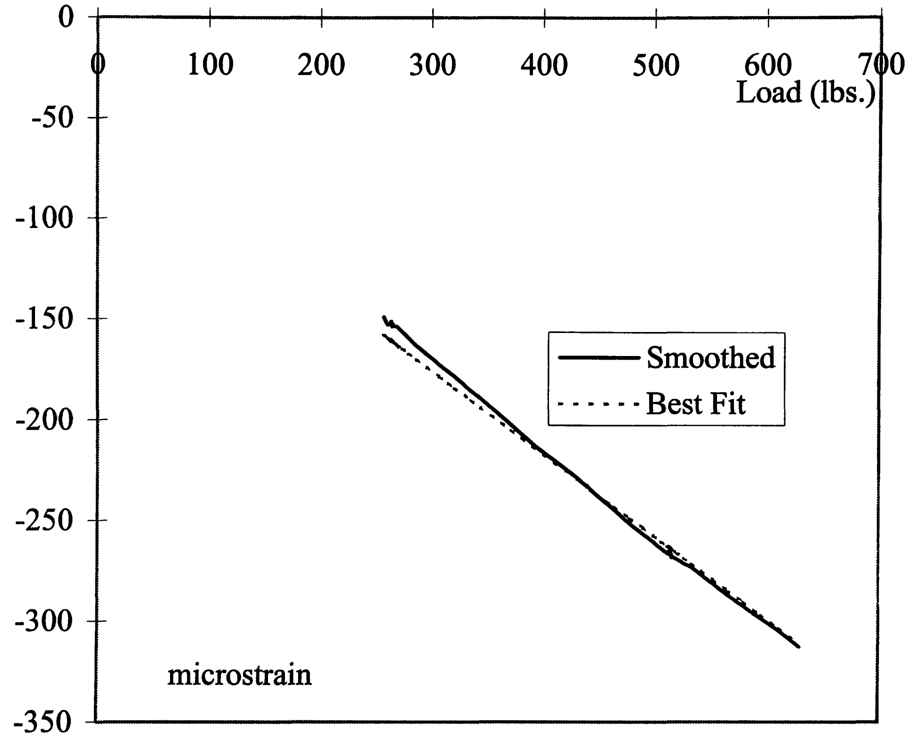

Figure 26. Load vs Strain, Smoothed & Linearized Data, Gage 4

Thirty seconds of data was recorded to allow sufficient time to hand pump the load up to 3000 lbs. At 50 Hz, with ten strain gages, and two load cell runs this produced 18,000 data points. Referring to Figure 24 which was a typical test run, the usable data was collected in approximately 20 seconds (150 lbs./sec). Raw data for one typical gage and the load cell reading can be viewed in Appendix A. The following table summarizes all the strain values and corresponding loads for the five load cases that were used in the analysis.

Gage	AXLE LOAD 600 lbs.	800 lbs.	1000 lbs.	1200 lbs.	1400 lbs.
1	157.1	209.63	262.14	314.66	367.18
2	-538.75	-701.12	-863.49	-1025.86	-1188.23
3	-447.79	-598.14	-748.49	-898.85	-1049.20
4	-416.99	-549.03	-681.07	-813.10	-945.14
5	19.77	36.54	53.32	70.10	86.88
6	364.00	492.25	620.50	748.75	877.00
7	184.41	251.67	318.93	386.18	453.44
Max Principal	376.64	508.49	640.35	772.21	904.07
Min Principal	-172.46	-220.27	-268.10	-315.93	-363.76
8	86.27	126.53	166.79	207.04	247.30
9	-232.43	-304.97	-377.50	-450.03	-522.57
10	-482.21	-641.21	-800.22	-959.22	-1118.22
Max Principal	88.35	129.47	170.60	211.71	252.84
Min Principal	-484.29	-644.16	-804.02	-963.89	-1123.75

Table 2. Experimental Microstrain

When processing a signal through small jumper wires to a solder pad, then through six foot lead wires to solder connections on the Wheatstone Bridge, into the Sensotec amplifiers, and finally through the IO Tech A/D board, some amount of error is expected. Attempting to determine the exact error range developed by this system is beyond the scope of this thesis.

In consideration of the potential error margin, Gages 1 through 4 produced adequate strain levels for comparison. Gage 8 and especially gage 5 were marginal. This may effect the comparison to the FEA data in the following chapters.

Rosette R1 measured strain values substantially less than gage U3 which was used to measure strain during the road test. This was expected. Both of these gages were located on the lower surface of the left arm at the elbow. However, they were not located at the same spot. The width of the beam at this location is approximately 1 inch. The gage locations were within 0.5 inches of each other, yet the strain levels are significantly different. Gage U3 was placed as close as possible to the corner of the 1x2 box section. Rosette R1 was almost centered on the 1 inch wide surface. These two gage readings as well as the fringe plots (not shown) identify a large magnitude of strain as well as a large strain gradient at this position along the arm.

Refer to Measurements Group's Tech Note 512, Plane-Shear Measurement With Strain Gages, for equations and description of technique to convert 45 degree rosette data into maximum and minimum principal strains.

6. Calculation Of Classical Data

Hand calculations were performed using classical methods to provide an additional check against one strain gage and the analysis results. Gage 1 was used for this check. Refer to Figure 27 for the location of the gage and surrounding geometry. Figure 28 illustrates the resultant load case at the gage location.

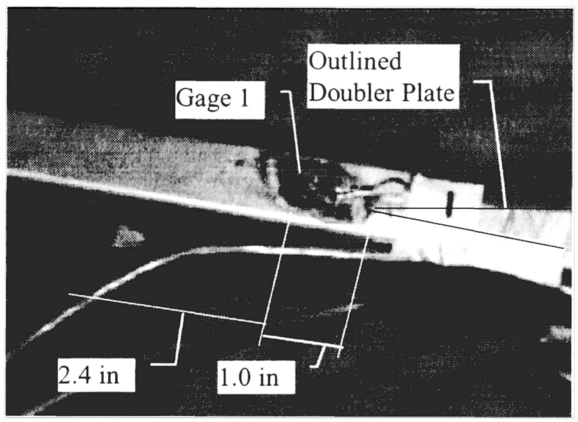

Figure 27. Gage 1 Location

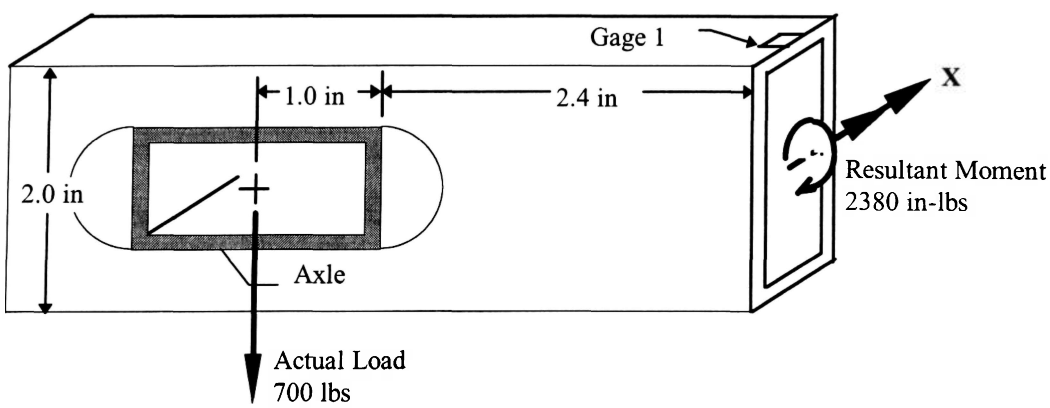

Figure 28. Load/Resultant Diagram

$$\varepsilon_{Gage1} = \frac{\sigma}{E} = \frac{Mc/I_X}{E} = \frac{Mc}{EI_X} \quad \text{where:}$$

M = resultant moment

c = distance from neutral axis to outer most fibers

E = Modulus of Elasticity

I_X = Area Moment of Inertia about X axis

The first step was to calculate the area moment of inertia for the beam cross section about the X axis. The cross section has been broken into three groups, the corners, the side rectangular sections, and the top and bottom rectangular sections (Figure 29).

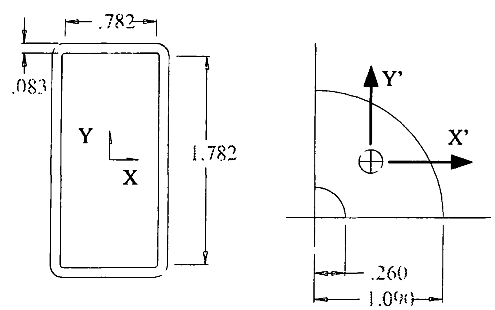

Figure 29. Cross Section of Swingarm

Area moment of inertia for the top and bottom sections about the local X' Axis:

$$I_{X'_{TB}} = \frac{1}{12}bh^3 = \frac{1}{12}(0.782\text{ in.})(0.083\text{ in.})^3 = 372.62e^{-7}\text{ in.}^4$$

Area moment of inertia for the side sections about the X axis:

$$I_{X_S} = \frac{1}{12}bh^3 = \frac{1}{12}(0.083\text{ in.})(1.782\text{ in.})^3 = 391.40e^{-4}\text{ in.}^4$$

Area moment of inertia for the corners about the local X' axis:

Centroid location using polar coordinates (Figure 30):

$$\bar{r} = \frac{\int_A \tilde{r}\,dA}{\int_A dA} = \frac{\int_0^{\pi/2}\int_{026}^{109} \tilde{r}\,dr\,d\theta}{\int_0^{\pi/2}\int_{026}^{109} dr\,d\theta} = \frac{\frac{1}{2}\left(.109^2 - .026^2\right)\frac{\pi}{2}}{(.109 - .026)\,\frac{\pi}{2}} = .0675 \text{ in.}$$

$$\bar{\theta} = \frac{\int_A \tilde{\theta}\,dA}{\int_A dA} = \frac{\int_0^{\pi/2}\int_{026}^{109} \tilde{\theta}\,r\,d\theta}{\int_0^{\pi/2}\int_{026}^{109} dr\,d\theta} = \frac{(.109 - .026)\,\frac{1}{2}\,\left(\frac{\pi}{2}\right)^2}{(.109 - .026)\,\frac{\pi}{2}} = \frac{\pi}{4}\ rad$$

$$\bar{x} = \bar{y} = (0.0675 \text{ in.})\sin\frac{\pi}{4} = 0.04773 \text{ in.}$$

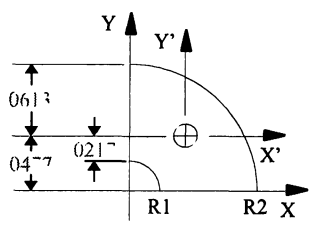

Figure 30. Local Axis

Translation of equations defining shape to centroid axes:

$$(x - x_0)^2 + (y - y_0)^2 = r^2$$

$$R_1\ (x + 0.04773)^2 + (y + 0.04773)^2 = 0.026^2$$

$$R_2\ (x + 0.04773)^2 + (y + 0.04773)^2 = 0.109^2$$

$$R_1\ x = \sqrt{0.026^2 - (y + 0.04773)^2} - 0.04773$$

$$R_2\ x = \sqrt{0.109^2 - (y + 0.04773)^2} - 0.04773$$

$$I_{X_{CR}} = \int_A Y^2\,dA$$

$$I_{X_{CNR}} = \int_{-0\,04773}^{-0\,02173} Y^2 \left\{ \left[\sqrt{0.109^2 - (y + 0.04773)^2} - 0.04773 \right] - \left[\sqrt{0.026^2 - (y + 0.04773)^2} - 0.04773 \right] \right\} dy + \int_{0\,02173}^{0\,04773} Y^2 \left\{ \sqrt{0.109^2 - (y + 0.04773)^2} - 0.04773 \right\} dy$$

$$I_{X_{CNR}} = 310.427e^{-4} \text{ in.}^4$$

Using the Parallel Axis theorem,

Combined area moments for the four corners about the X axis:

$$I_{X_{CNR}} = 4\langle I_{X'} + Ad^2 \rangle = 4\langle 565.99e^{-8} + \tfrac{\pi}{4}(0.109^2 - 0.026^2)(0.93873)^2 \rangle$$

$$I_{X_{CNR}} = 310.427e^{-4} \text{ in.}^4$$

Combined area moments for the top and bottom sections about the X axis:

$$I_{X_{TB}} = 2\langle I_{X'} + Ad^2 \rangle = 2\langle 37.261e^{-6} + (0.782)(0.083)(0.9585)^2 \rangle$$

$$I_{X_{TB}} = 119.336e^{-3} \text{ in.}^4$$

Summing all area moments:

$$I_{X_{TOTAL}} = I_{X_{CNR}} + I_{X_{TB}} + 2I_{X_S} = 310.427e^{-4} + 119.336e^{-3} + 2(391.398e^{-4})$$

$$I_{X_{TOTAL}} = 228.658e^{-3} \text{ in.}^4$$

$$\varepsilon_{Gage1} = \frac{\sigma}{E} = \frac{Mc/I_X}{E} = \frac{Mc}{EI_X} = \frac{(700lbs)(3.4in)(1in)}{(30e^6)(228.658e^{-3})}$$

$$\varepsilon_{Gage1} = 346.95\,\mu\varepsilon$$

While being the most suitable for a hand calculation, as shown in Figure 27 this gage location still violates Saint-Venant's principle which indicates a questionable level of accuracy when using theoretical equations within one maximum material dimension from a fixed end or other change in geometry (Beer, 78). Along the arms of the swingarm, the maximum dimension is 2 inches. Gage 1 is 2.4 inches from the axle, and within 1 inch of the tip of the doubler plate. Despite these cautionary statements, the calculated strain value of 347 με provides a reassuring sanity check when compared with the measured value of 367 με from Table 2, a difference of only 5.4%

7. Computation Of GEM/FEA Data

7.1 General Background on Pro/Mechanica Analysis

Structural analysis software traditionally uses the finite element method to build and analyze a geometric model of a part. According to this method, the part is divided into small finite elements. Pro/Mechanica uses high-order finite elements, called geometric elements, to simulate the static or dynamic elastic deformation of mechanical parts.

Geometric elements are based on what is called the p-version of the finite element method, or p-method. The p-method represents the displacements within each element using high-order polynomials, as opposed to the linear and sometimes quadratic or cubic functions used in conventional finite elements. As deformation of the element edges increases in magnitude and complexity, higher order equations can approximate the edge shape better. A single geometric element can therefore represent a more complex state of deformation than a single, conventional finite element (King).

Pro/Mechanica automatically solves the equations for the model with successively higher-order polynomials, up to ninth order, until the percent change or convergence between the results of the last two calculations is within a user set criterion. This approach provides assurance that the results are accurate.

The software enables the user to define his/her own design variables, such as material thickness, or the radius of a hole or fillet. The geometric elements can have curved edges, are insensitive to distortion, and are automatically associated with the underlying geometry; when a design variable changes, the elements change accordingly. The user can change the design variables for sensitivity and optimization studies. In sensitivity studies, Pro/Mechanica provides data over a specified range of the design variables, or at specified values.

In optimization, one of two search algorithms (gradient projection or sequential quadratic) are used to find the values of the design variables that satisfy the user requirements. This allows the user to perform design studies that, for instance, reduce material thickness until a specific stress level is reached.

7.2 The Analytical Model

The model was created using the geometry package that comes standard with Pro/Mechanica. Of the three element types available in Pro/Mechanica, beams, shells, and solids, the thin walled sections used for the various components of the swingarm assembly are most suitable for shell type elements. These are created as two dimensional (2D) surfaces with a material thickness assigned to them. During the analysis, the assigned material thickness defaults to an equal distribution on each side of the 2D shell element. To accommodate for dimensional effects generated by this material thickness distribution method, the part was modeled by its midplanes. Figure 31 illustrates the complete analysis model.

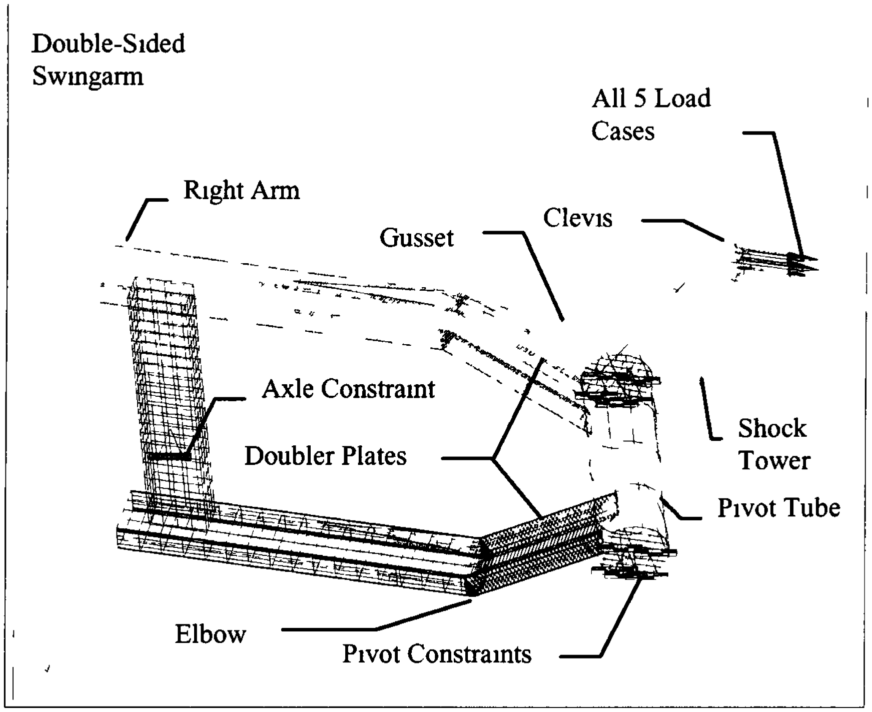

Figure 31. Analysis Model

The manufacturing process of the bends in the arms of the swingarm begins by cutting a wedge shape out of the inside of the arm. The outside wall of the tubing is left intact. The bend is formed by bending this outside wall until the wedge shape cutout is eliminated (Figure 32). A full penetration weld bead is applied along the three butted surfaces. Since this weld bead effectively serves as a fillet, the analysis model was filleted on the inside edge as shown.

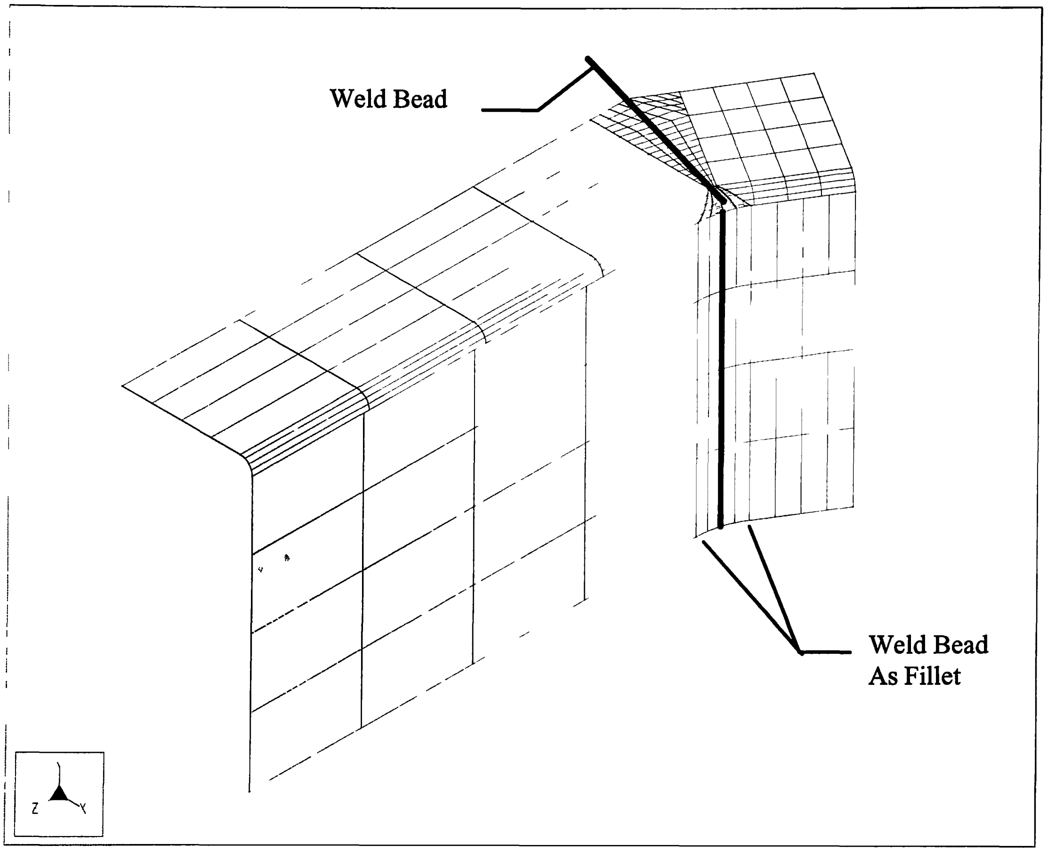

Figure 32. Weld Bead Fillet

The doubler plates along the lower surface of the arms are stitch welded on production parts. The first model defined the adjoining areas with double material thickness equal to the combined thicknesses of the doublers and the tubing wall. No additional material was added for the welds. This is similar to a continuous weld along the edges or a furnace braze technique. The stitch welds also were modeled as elements between the raised doublers at their midplane and the wall of the swingarm tube (Figure 33). However, the results were only marginally affected by the different modeling technique. Modeling of the welds was an area of serious concern which turned out to be not critical.

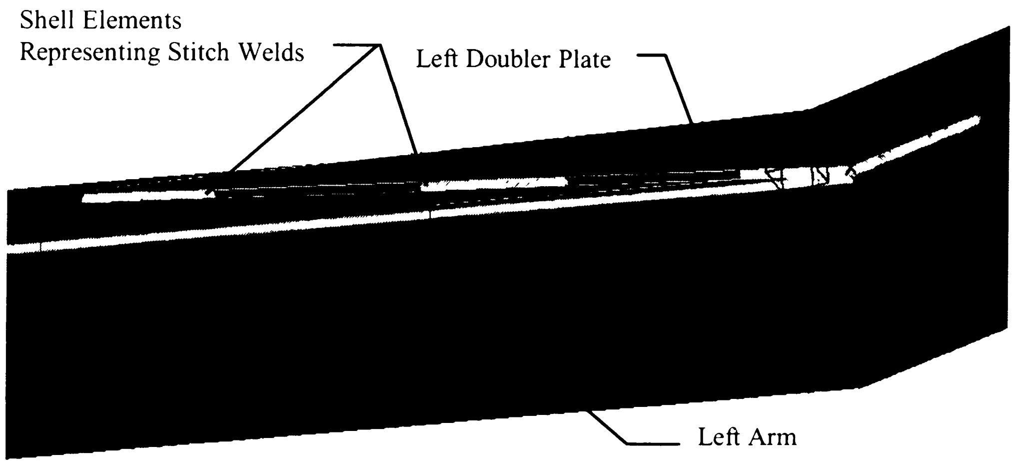

Figure 33. Stitch Weld Modeling Technique

The axle was modeled as a 1x2x.083 wall tube spanning the two arms. The connections at the belt adjustment slots in the arms were continuous at the point of contact. A constraint was placed on a surface equivalent to the washer diameter used in the laboratory setup. With the exception of the continuous connection at the belt adjustment slots, this matches the laboratory setup exactly (Figure 16). The continuous connection, associating the bordering elements with each other, simulates a welded joint with no additional material added. The laboratory setup was not welded. However for the load and geometry used, a welded connection would not have affected the results.

The Contact module of Pro/Mechanica could have been used to model this connection exactly. In consideration of the proximity of the joint to the strain gages, this was not necessary.

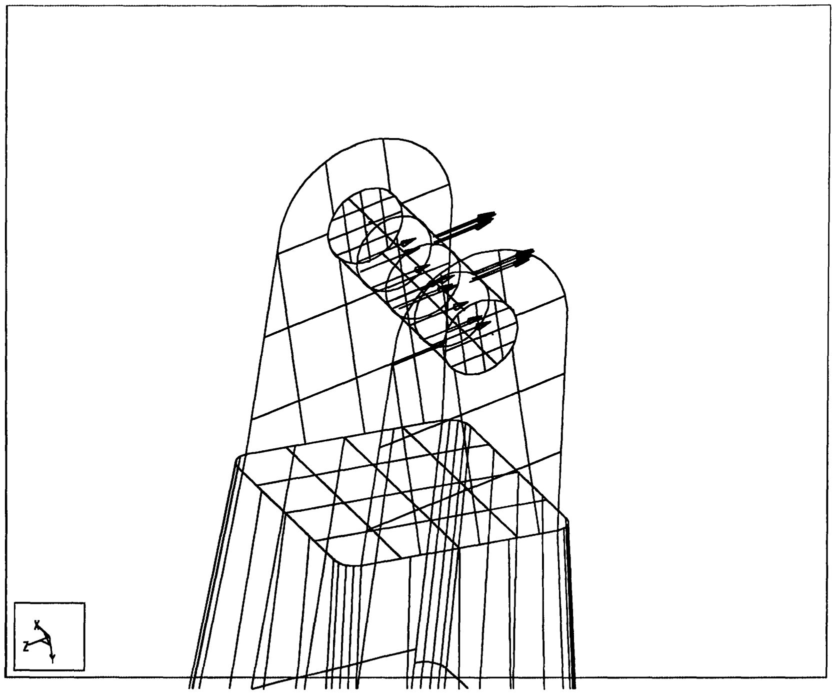

Figure 34. Load Point At Clevis Pin

Referring to Figure 34, the load was applied to a cylinder representing the fastener that passes through the clevis on the shock tower. Ideally, locations for loads should be chosen in an order of preference of surface, edge, point. Applying a load at a point produces an infinite stress concentration. For modeling purposes, sometimes an infinite stress at a point is acceptable. To avoid lengthy run times, the element edge order (order of the polynomial used to represent the edge shape) on the elements surrounding the point should be restricted to 2 or 3. This will stop the analysis from performing successive passes on this point up through element edge order of 9 in an attempt to get convergence. This reduces the time consumed on computing the infinite stresses that theoretically accompany a point load. An edge constraint does not require the element edge order constraint. However, a surface load would be best. Figure 35 illustrates the user interface for defining loads.

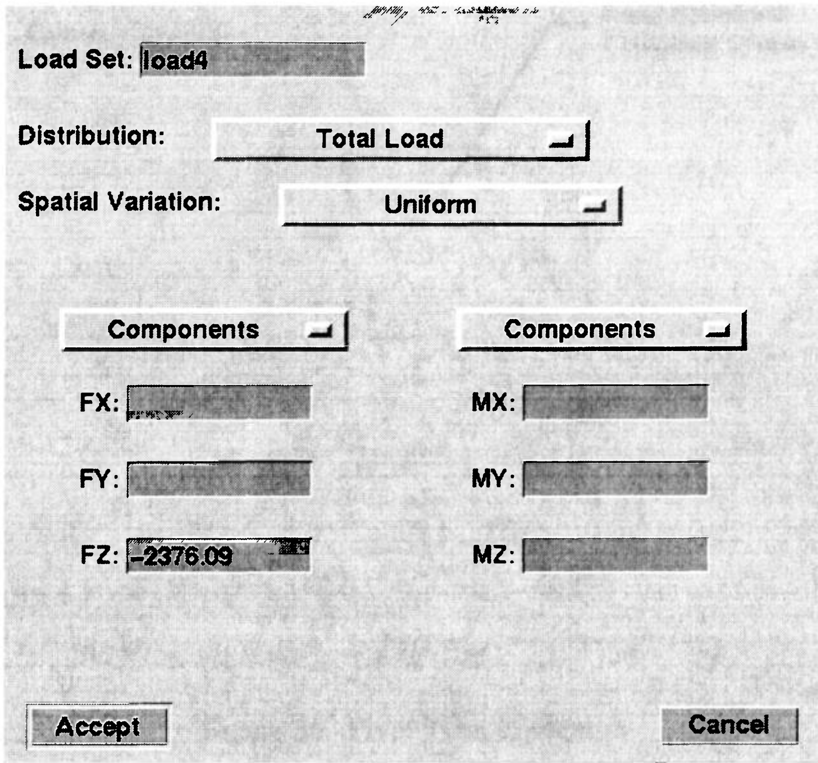

Figure 35. User Interface For Defining Loads

The constraints for the pivot were developed using local cylindrical coordinates. The Z axis lies along the center of the tube. Displacement in the theta direction and rotation about the Z axis were free. All other displacements and rotations were fixed (Figure 36).

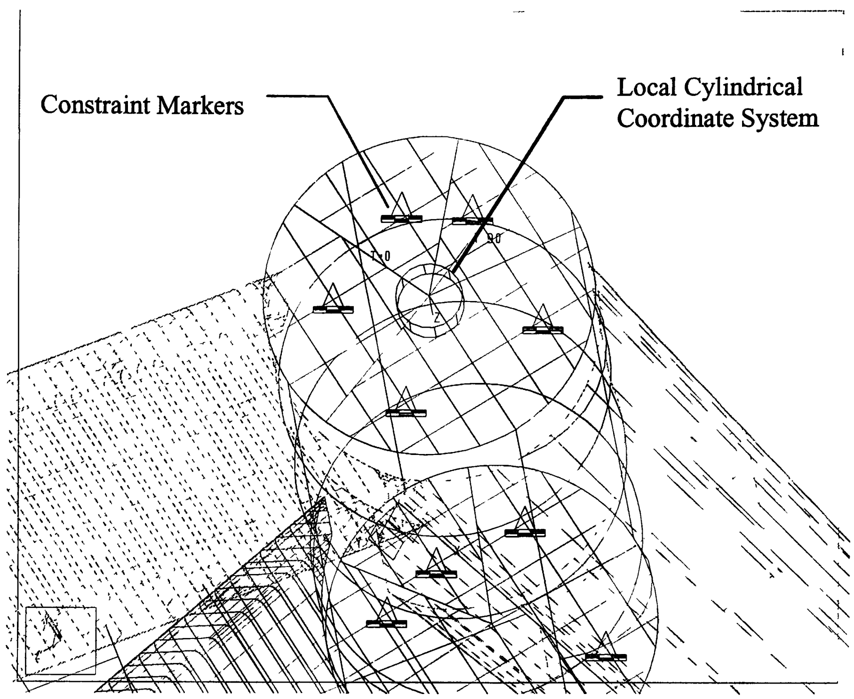

Figure 36. Pivot Tube Constraint

The axle was constrained using this same coordinate system as well. By restricting displacement in the theta direction and rotation about the Z axis, the axle was fixed in space in relation to the load applied at the clevis. The displacement in the R direction was also left free. This allowed small deflections due to bending over the length of the swingarm to be unconstrained.

The constraint options provided for all coordinate systems, cartesian, cylindrical, and spherical, are the same. These constraints are 'fixed' or 'free' in displacement and rotation about each of the axis (Figure 37). For cylindrical and spherical coordinate systems, this produces some unusual constraints. Considering cylindrical coordinates, displacement in the theta direction and rotation about the Z axis are the same. The user must realize this and set these two parameters to be the same. Additionally, rotation about the theta axis is a constraint that may never be used. This would be a radial line intersecting a circle then rotating about the circle perpendicular to the tangent line at the point of intersection. The spherical coordinate system has some equivalent concerns when picking constraints. Figure 38 illustrates and defines the constraint markers used in Pro/Mechanica. A fixed condition would be indicated by a solid block.

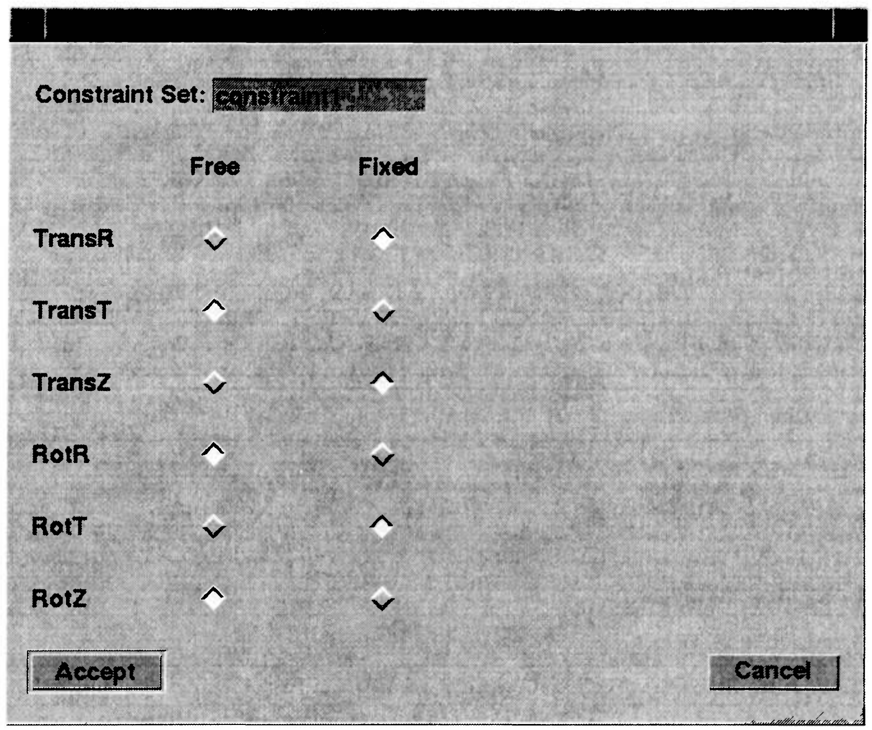

Figure 37. Constraint Window, Cylindrical Coordinates

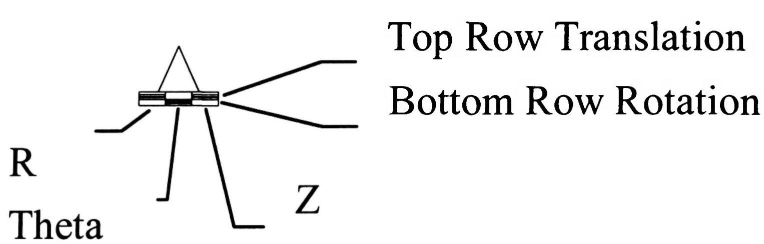

Figure 38. Pro/Mechanica Constraint Marker, Cylindrical Coordinates

Once the geometry has been created, material properties are assigned. These can be assigned to the shell elements, or to the underlying geometry. Assigning the properties to the geometry is recommended. This allows mesh changes without redefining material properties. Figure 39 illustrates the window used for defining material properties.

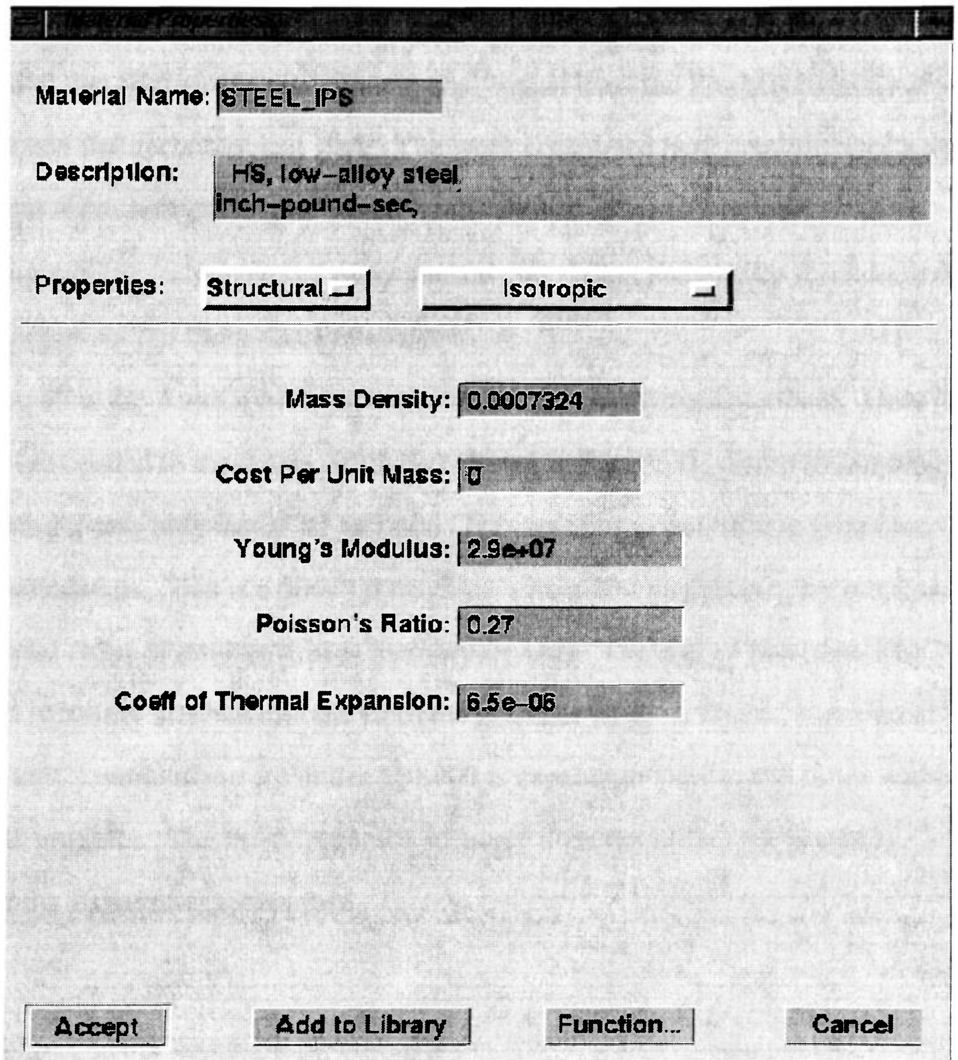

Figure 39. Material Properties Window

7.3 Mesh Creation

The original element mesh was generated by the Pro/Mechanica AutoGEM feature. Once the surface geometry has been created, the AutoGEM routine can be initiated for any or all surfaces on the model. PTC, the software manufacturer, has been promoting this feature with the intent that any designer can create the model, apply loads and constraints, AutoGEM the element mesh, and run the analysis. The results of this thesis document that this feature of finite element analysis, at least the Pro/Mechanica software, has not reached that technological state. The work completed here demonstrates a need for additional mesh refinement performed by the analyst in areas where accuracy is desired. Engineering judgment and experimental correlation techniques should always be used to complement the finite element analysis.

Figure 40 is the AutoGEM Summary window for the swingarm model. Only 793 elements were needed to mesh this entire part shown in Figure 31. More astounding is that the mesh process only lasted 54 seconds. This was done on a Silicon Graphics Indigo II workstation. This is a $30,000 machine with a 200 megahertz processor and 224 megabytes (Mb) of random access memory (RAM). The cost of this particular workstation is mainly attributed to the Extreme graphics card. A Digital Equipment Company (DEC) workstation for under $10,000 is capable of similar run times without the high end graphics. The Pro/Mechanica software does not utilize the graphics potential of the Extreme graphics card.

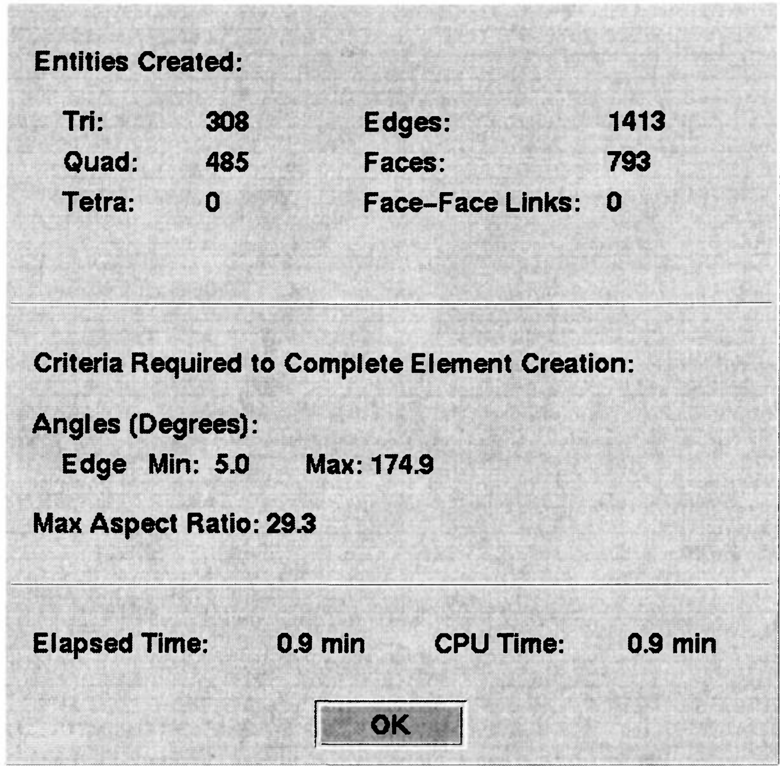

Figure 40. AutoGEM Summary Window

7.4 Analysis Techniques

The analysis uses the default settings as shown in Figure 41. Note the convergence criteria was left at the default setting of 10%. This is user defined, and can be set as low as 1%. Convergence is attained when the difference in the results of the current pass and the previous pass are within the percentage specified (Design Study Reference, 14).

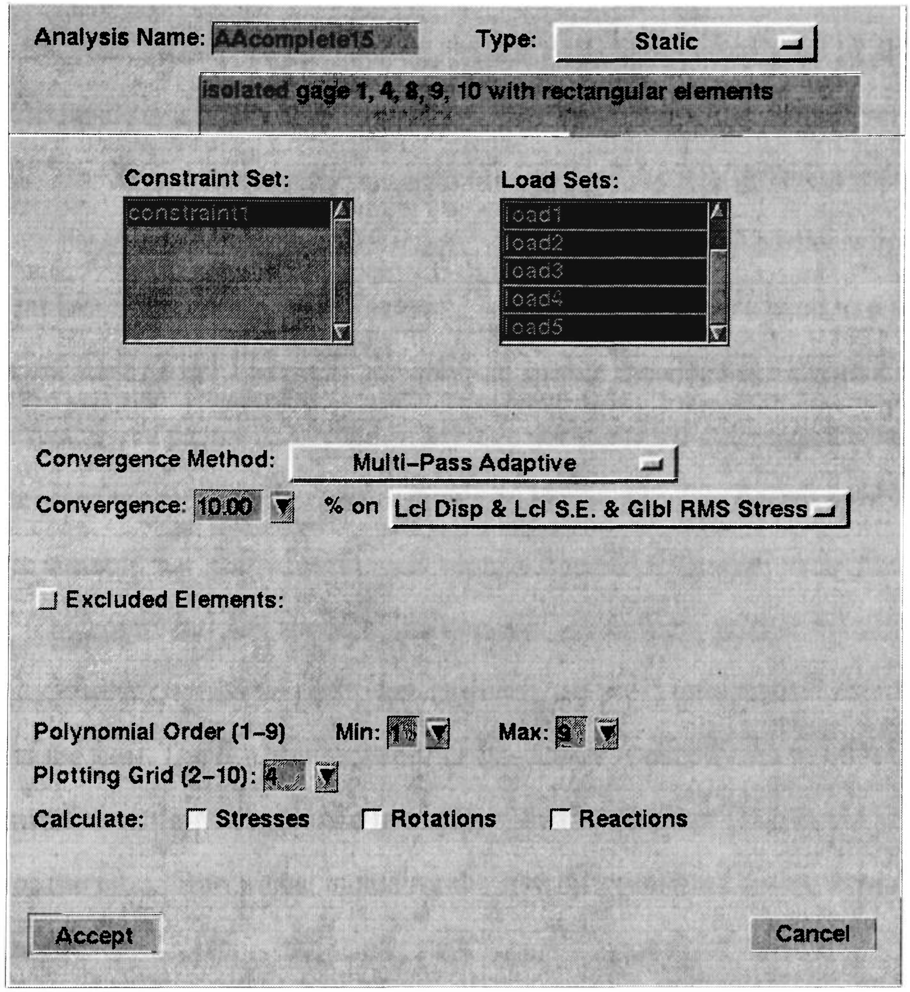

Figure 41. Analysis User Interface

This parameter was not varied for this project mainly due to the increase in run times lower settings produces. Test cases using 10% and 25% convergence yielded only 5%-10% variance in maximum solution values for the various results. These small changes in maximum values are accompanied by substantial run time reductions. During each pass, the analysis engine solves equations for all elements which have not yet satisfied the convergence criteria. When a pass is completed, the equations for elements that satisfy the convergence criteria are no longer included in the matrix. This means elements removed in earlier passes reduce analysis time for every pass they would have been in after that point. Based on this finding, the convergence is usually set to 20% unless a specific location merits closer evaluation. For this project, the default value of 10% was used. The five different load sets represent each of the five different load cases evaluated. Note the excluded elements selection. This was referenced earlier when discussing point loads and constraints. Elements are selected to be restricted to a user specified element edge order. Normally the analysis engine increases the element edge order through successive passes as needed to achieve the specified convergence criteria.

The user interface for Run Settings is shown in Figure 42. The iterative solver offered is more suitable for 'chunkier' models usually meshed with solid elements (Sporzynski). The computational speed of the iterative solver is far greater than the block solver. The block solver, while being slower, provides the most information about the convergence of the run. The RAM allocation for the Solver is usually set to 60% of the machine's total ram or 146 Mb as shown in Figure 42. The Element Data RAM is set to 10% (24Mb) of the total. Run times, including the five different load cases, were on the order of four hours.

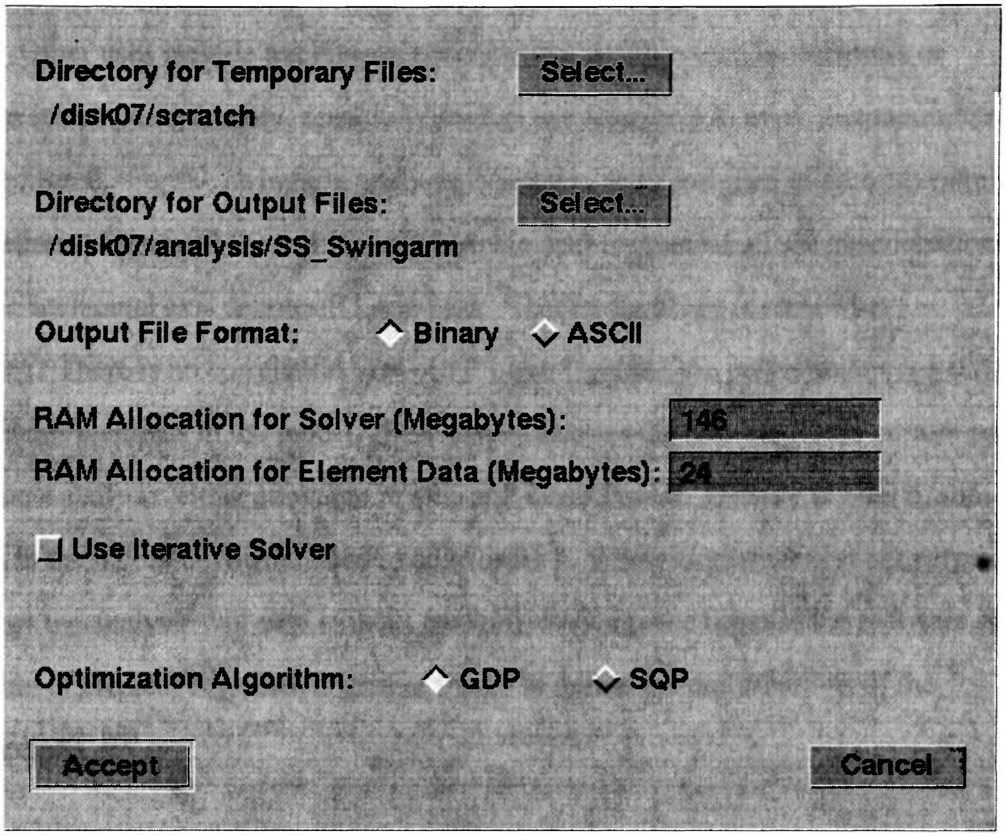

Figure 42. User Interface, Run Settings

Once the analysis has been defined and the run is ready to be started, the software performs an error checking routine. This highlights all the element edges, identifies the need for links, locates any breaks in the shell elements, checks that material properties exist for all elements, etc.

After the run has completed, the convergence plots are checked. Unless Measures have been defined, the default setting only tracks the convergence at the location of maximum stress. A measure is a scalar quantity of interest that Pro/Mechanica calculates during a specific design study (Parametric, 298). Directing the Pro/Mechanica engine to focus on a specific location or parameter of the model provides a number of uses to the analyst. In this case it is used to monitor the convergence of the analysis run at a specific location. Other uses include tracking an optimization variable such as thickness or maximum stress. Additionally, sensitivity studies use Measures to mark the parameters being monitored. For the swingarm analysis, Measures were assigned to all of the strain gage locations. Figure 43 through 48 illustrate the convergence of all six gage locations.

The horizontal axis denotes P Loop Pass. This terminology is somewhat misleading. There is no correlation between P Loop Pass and the polynomial edge order of the various elements in the model. This simply denotes the number of the current pass. In fact, most analyses either converge or stop at P Loop Pass 6. Usually at Pass 6, some elements in the model have graduated to edge order 9. These elements must converge on this pass or the analysis will stop without reaching convergence because the software is not capable of element edge orders greater than 9 to define the deformations of the element edges.

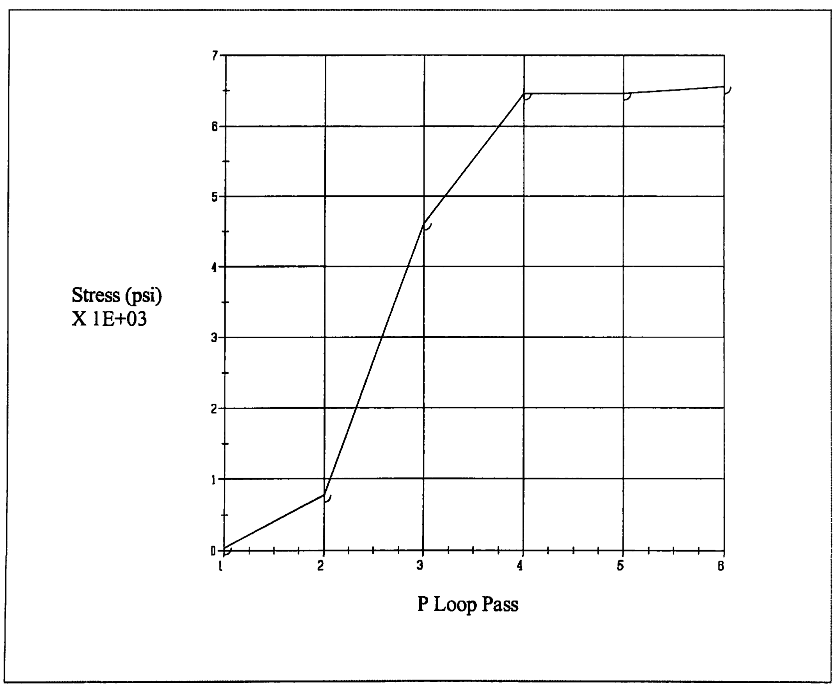

Figure 43. Convergence Plot, Gage 1, Load = 1400 lbs.

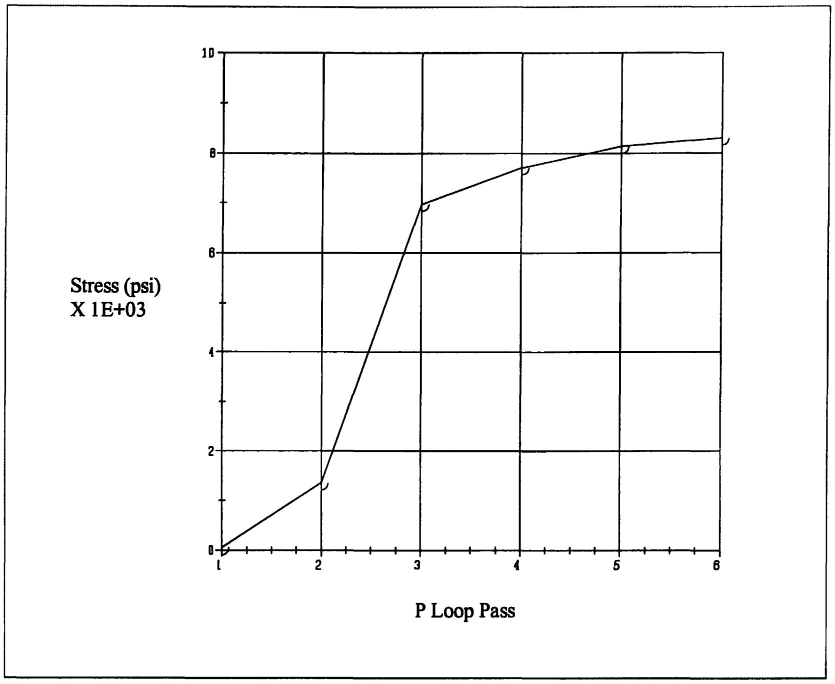

Figure 44. Convergence Plot, Gage 2, Load = 1400 lbs.

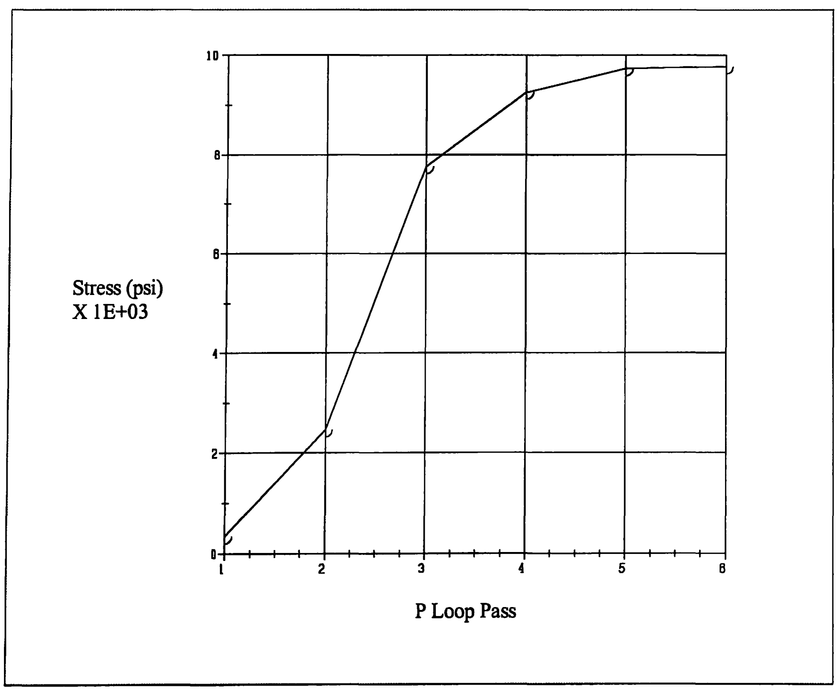

Figure 45. Convergence Plot, Gage 3, Load = 1400 lbs.

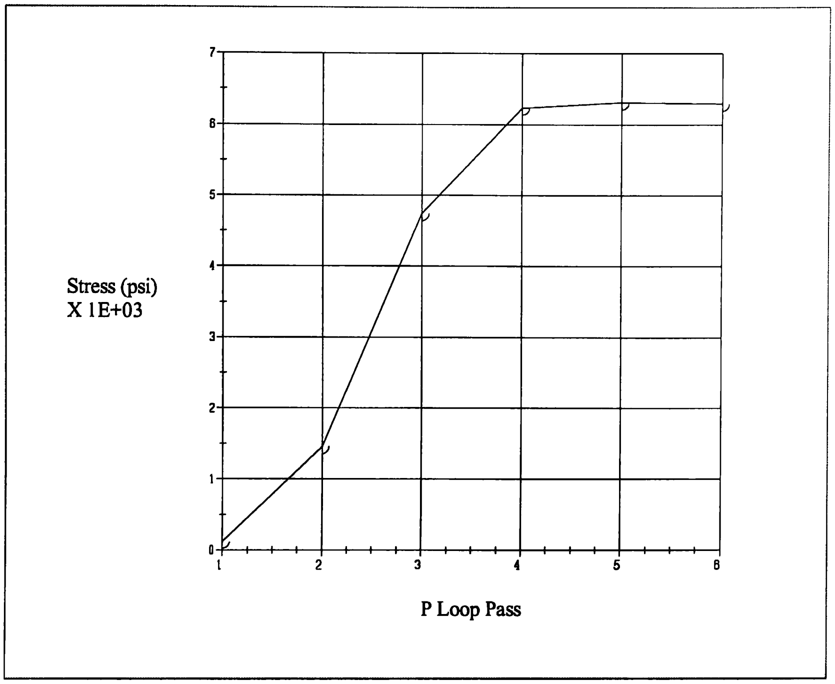

Figure 46. Convergence Plot, Gage 4, Load = 1400 lbs.

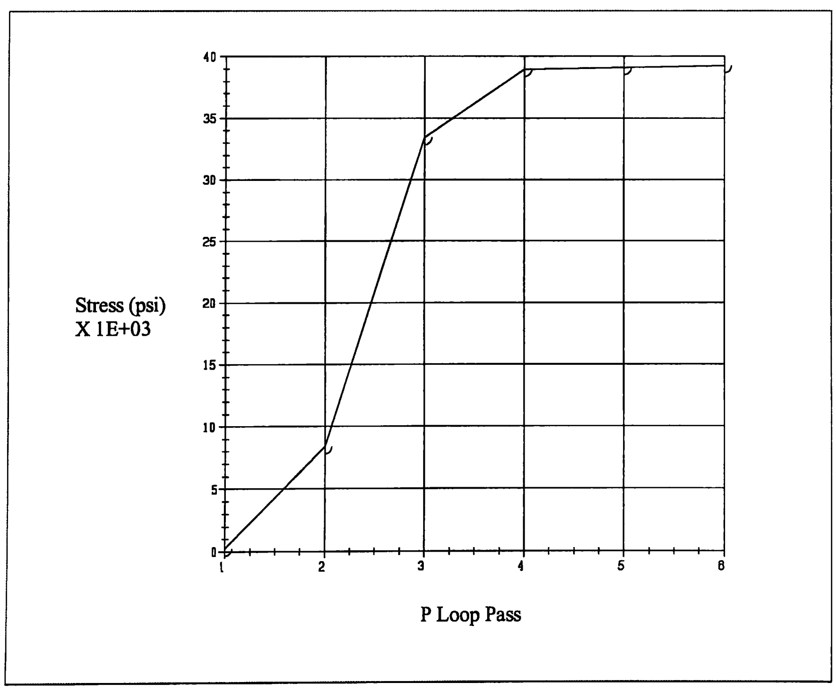

Figure 47. Convergence Plot, Gage R1, Load = 1400 lbs.

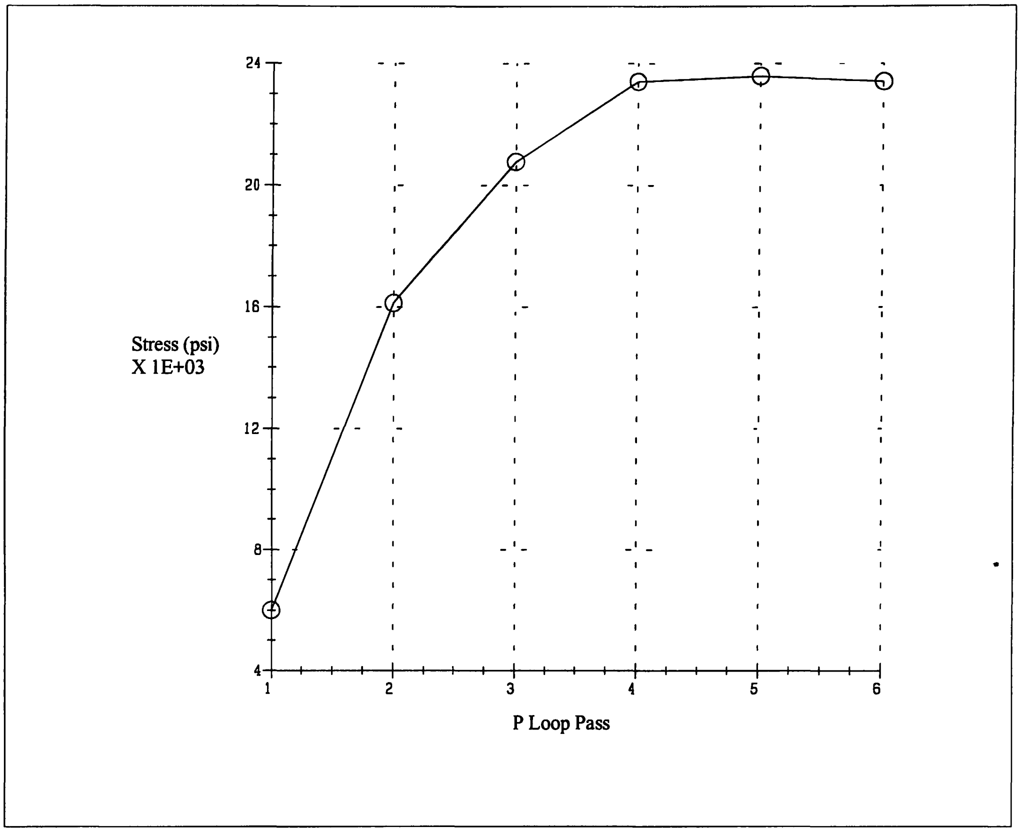

Figure 48. Convergence Plot, Gage R2, Load = 1400 lbs.

7.5 Extract Strain Data From Result Files

The result files for an analysis run contain a large amount of information and multiple ways for viewing/reviewing it. Figure 49 depicts a freeze frame of the animation results. The deflections are uniformly amplified and animated in negative and positive directions. This display method is helpful in identifying improper constraints.

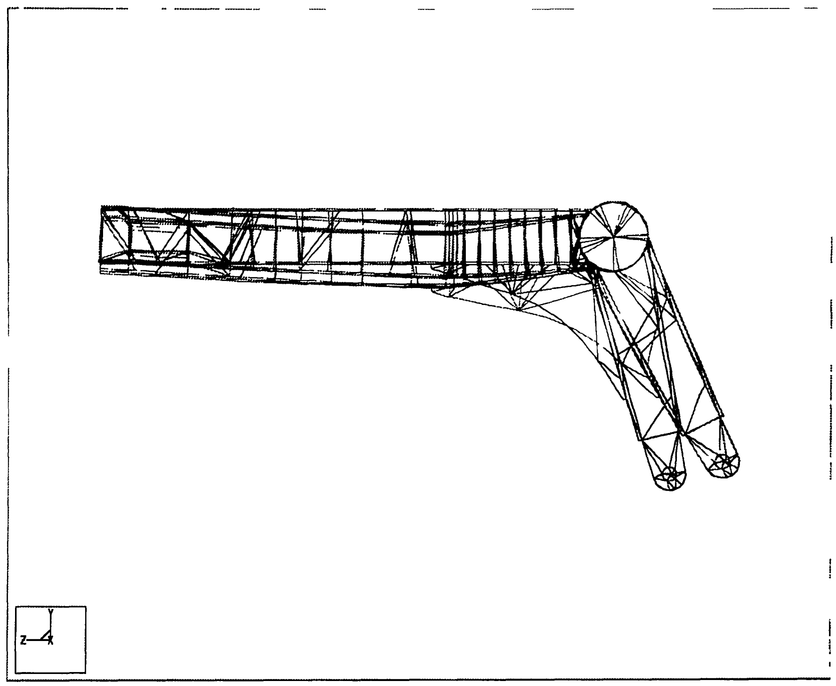

Figure 49. Animated Displacement Results

Of the multiple ways to view strain results from an analysis run, the simplest method displays strain along an axis relative to the world coordinate system. The reference can also be switched to material orientation. Referring to the Parametric Technology Corporation's Pro/MECHANICA Model Reference for Structure and Thermal, if not assigned by the user, the three material orientations are defined by the parameterization of the surface. Material direction 3 is perpendicular to the surface and aligned with the surface normal. Material direction 1 is parallel to the first parameter curve of the surface. Material direction 2 is set perpendicular to directions 1 and 3. (191) Maximum principal strain is also available. However, when using shell elements the software defaults to whichever side of the element the maximum occurs on. This is the same for minimum principal strain as well. There is no method for selecting a specific side, like the side the strain gage is mounted on. Due to this limitation, principal strains had to be computed by hand from individual strains measured in the XX, YY, and XY directions.

A query plot was used to identify the strain values for the individual gage locations. For all the gages except R1, a single grid point was centered under the gage. Figure 50 displays the grid underlying R1. Each point on the grid was queried and the values averaged for each axis to produce the principal strain data.

Preliminary work was done to determine if element corners coming together under the gage location produced results different than averaging the grid on one element under the gage. There was no significant difference in the results. The R1 rosette location was modeled with an element grid because it required the least amount of work modifying the element mesh in the area. Hand meshing is possible, but still very time consuming.

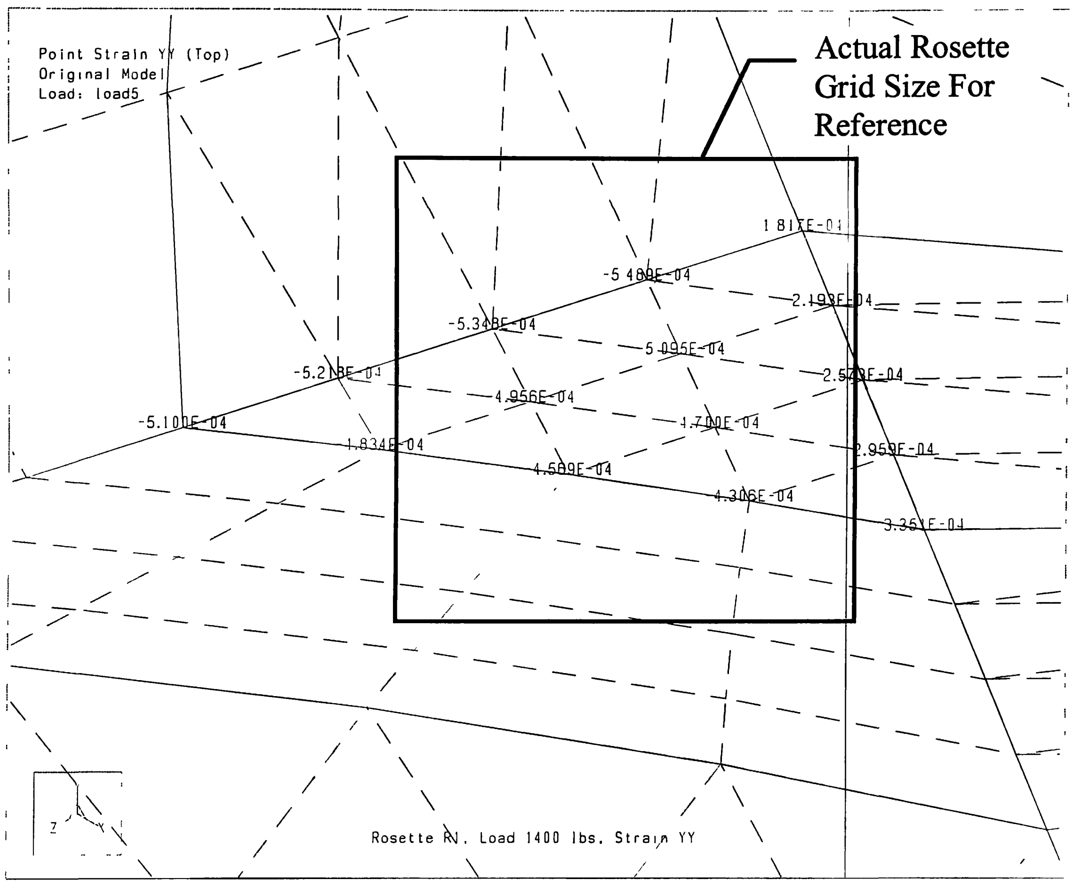

Figure 50. Query Plot, Rosette R1, Load = 1400 lbs.

Table 3 lists the microstrain values for each gage at each load. The values on the XX, YY, and XY axis do not correlate to the values in Table 2. The rosette orientation and the software's element orientation were not the same. The comparison of these results with those in the preceding chapters follows in Chapter 8.

Gage Location	AXLE LOAD 600 lbs.	800 lbs.	1000 lbs.	1200 lbs.	1400 lbs.
1	48.12	64.16	80.19	96.23	112.30
2	-512.10	-682.8	-853.4	-1024	-1195
3	-385.80	-514.5	-643.1	-771.7	-900.3
4	-511.7	-692.5	-865.6	-1039	-1212
5,6,7 - XX	435.83	581.10	726.37	871.73	1016.89
5,6,7 - YY	-104.92	-139.88	-174.87	-209.83	-244.81
5,6,7 - XY	-103.00	-137.77	-172.21	-206.66	-241.11
Max Principal	546.47	728.93	911.15	1093.49	1275.59
Min Principal	-215.56	-287.71	-359.65	-431.59	-503.51
8,9,10 - XX	-89.25	-119.0	-148.8	-178.5	-208.3
8,9,10 - YY	-88.79	-118.4	-148.0	-177.6	-207.2
8,9,10 - XY	396.2	528.3	660.30	792.4	924.5
Max Principal	396.20	528.30	660.30	792.40	924.50
Min Principal	-574.24	-765.70	-957.10	-1148.5	-1340.0

Table 3. Theoretical Microstrain

8. Comparison Of Strain Data From Initial FEA Model

Three different methods have been used to determine strain on the swingarm. With the nature of strain gage data and the checks imposed while taking the data, the strain gage readings are considered to be the most accurate. Using the strain gage data as the actual readings and the hand calculated or FEA data as the experimental parameter, the following equation will be used to determine percent difference for the total data set.

$$\%\,\text{Difference} = \left|\frac{\text{Actual} - \text{Experimental}}{\text{Actual}}\right| \times 100$$

$$\%\,\text{Difference} = \left|\frac{\text{Strain Gage} - \text{Theoretical / Classical}}{\text{Strain Gage}}\right| \times 100$$

8.1 Experimental vs Calculated and Theoretical

From Chapter 5, Table 2, the strain measurement for Gage 1 at the 1400 lb. load is 367.18$\mu\varepsilon$. From Chapter 6 the calculated strain is 346.95$\mu\varepsilon$.

$$\%\,\text{Difference} = \left|\frac{367.18\,\mu\varepsilon - 346.95\,\mu\varepsilon}{367.18\,\mu\varepsilon}\right| \times 100 = 5.5\%$$

From Chapter 7, Table 3, the strain is 112.30$\mu\varepsilon$.

$$\%\,\text{Difference} = \left|\frac{367.18\,\mu\varepsilon - 112.30\,\mu\varepsilon}{367.18\,\mu\varepsilon}\right| \times 100 = 69.4\%$$

The results demonstrate excellent correlation between the experimentally and the classically derived data. There is a substantial difference between these data and the theoretically derived value from the FEA package. This was not expected. Due to the close proximity of the axle and the doubler plate features, the classically derived data seems most likely to differ from the other two values. Strain gages inherently include the influence of surrounding geometry. The FEA analysis is not supposed to be susceptible to errors imposed by bordering geometry, but it may require an elaborate element mesh to model geometry changes adequately. This will be discussed further in Chapter 9, and became a major effort in the software verification process.

8.2 Experimental vs Theoretical

Table 4 is formatted identical to Tables 2 and 3. Percent differences are used in place of the strain readings. Note, these values are the percent differences taken before any element remeshing was performed.

Gage Location	AXLE LOAD 600 lbs.	800 lbs.	1000 lbs.	1200 lbs.	1400 lbs.
1	69.4%	69.4%	69.4%	69.4%	69.4%
2	4.9%	2.6%	1.2%	0.2%	0.6%
3	13.8%	14.0%	14.1%	14.1%	14.2%
4	22.7%	26.1%	27.1%	27.8%	28.2%
R1, Max Principal	45.1%	43.4%	42.3%	41.6%	41.1%
R1, Min Principal	25.0%	30.6%	34.1%	36.6%	38.4%
R2, Max Principal	348.5%	308.1%	287.1%	274.3%	265.7%
R2, Min Principal	18.6%	18.9%	19.0%	19.2%	19.2%

Table 4. Percent Difference, Experimental vs Theoretical

With only a 5.5% percent difference between classical and experimental values, the theoretical strains for gage 1 are suspect. Both gages 1 and 4 demonstrate unacceptable correlation. These locations, as well as rosette R1, are focused on in Chapter 9. Various modifications to the model have been attempted to reach acceptable correlation.

It is important to note that gages 2 and 3 are located at the elbows. These are areas with substantial stress gradients. To be able to mount a uniaxial gage alongside the highest stress point on the part and come within 15% of the theoretical results of the FEA model is significant.

9. Correlate Model To Experimental Strain Data

Chapter 8 determined the correlation of the strain gage readings to the analysis results for the first analysis run. Some of the gages were significantly different than the analysis results. The initial check is the convergence plot. All of these gages had good convergence. This prompted a discussion in a session of the Mechanica Users Group. Other companies using the Pro/Mechanica software had found that hand meshing around strain gage locations provided better correlation. By adding a ring of rectangular elements around the point being checked for correlation, a simpler deformation field is established. This generally produces lower polynomial orders on the element edge orders which should improve the accuracy of the analysis.

9.1 Gage 1

The original AutoGEM mesh that was created was modified slightly to provide the edges of the elements under the gage location (Figure 51). Once again, the initial run was set using default values wherever possible. The intent was to perform the simplest analysis run. Table 4 lists the experimental and theoretical strains as well as the percent difference. Figure 52 shows the hand meshing that was done for analysis Run 2. The refined mesh did affect the results. This in and of itself is noteworthy. For the Pro/Mechanica software the use of the P-method is not supposed to require hand meshing.

Additional mesh refinement may improve the results further. However, the theoretical values are one third the experimental data. Due to the proximity of the axle, further investigation would be directed at determining whether the axle modeling is accurate. Test cases would need to be run to isolate the critical load paths from the axle into the swingarm.

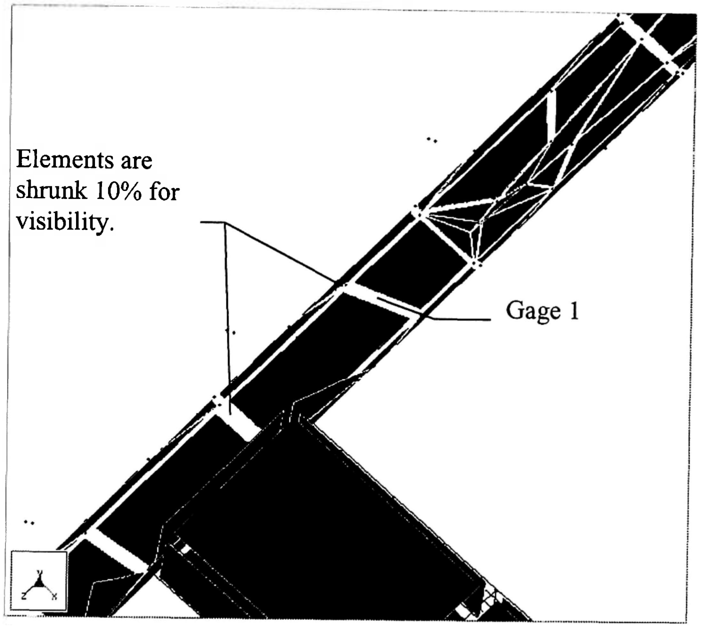

Figure 51. Gage 1 Shell Elements, Analysis Run 1

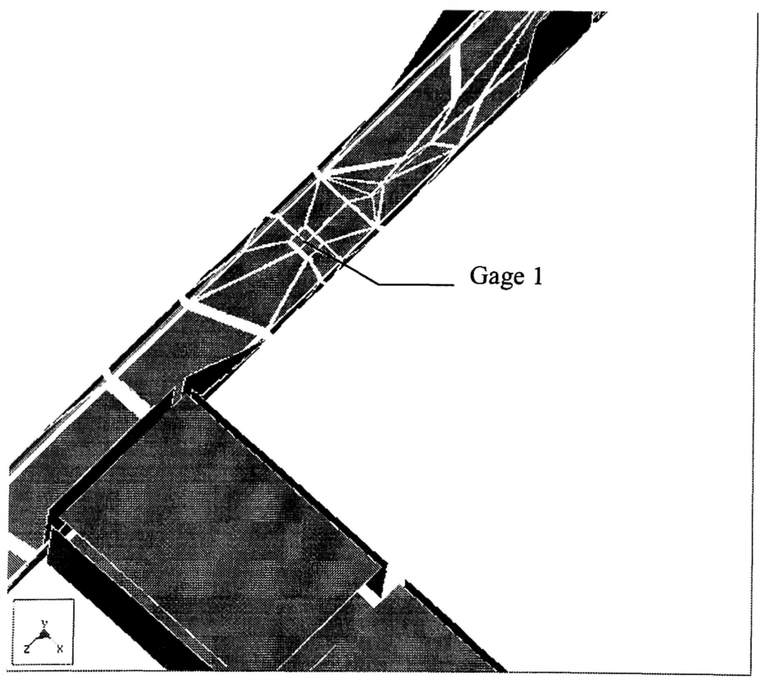

Figure 52. Gage 1 Remeshed Shell Elements, Analysis Run 2

Load	Exp. Strain	Run 1	% Diff.	Run 2	% Diff.
600 lbs.	157.11	48.12	69.4%	56.9	63.8%
800 lbs.	209.63	64.16	69.4%	75.87	63.8%
1000 lbs.	262.14	80.19	69.4%	94.84	63.8%
1200 lbs.	314.66	96.23	69.4%	113.8	63.8%
1400 lbs.	367.18	112.3	69.4%	132.9	63.8%

Table 5. Experimental vs Theoretical Strain, Gage 1

9.2 Gage 4

The same mesh refining procedure was performed on Gage 4. The strain gage location was isolated within two rings of clean, rectangular elements. This is done to facilitate the analysis engine in computing the polynomial equations that best represent the deformation of any two joining elements. The P-method is capable of handling curved edges of three dimensional surfaces with extreme edge angles. It is not necessarily optimal to do this though as demonstrated by the data in Table 5. The data from Run 1 to Run 2 went from an average of 25% to 10% difference from the experimental data.

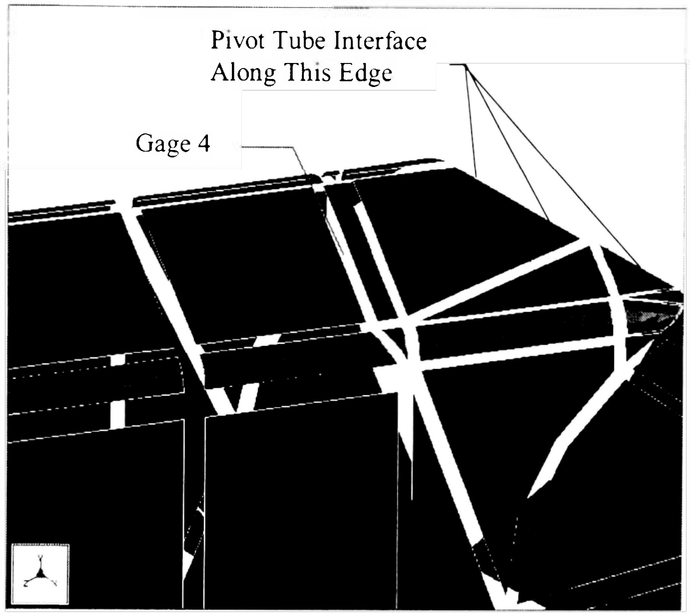

Figure 53. Gage 4 Shell Elements, Analysis Run 1

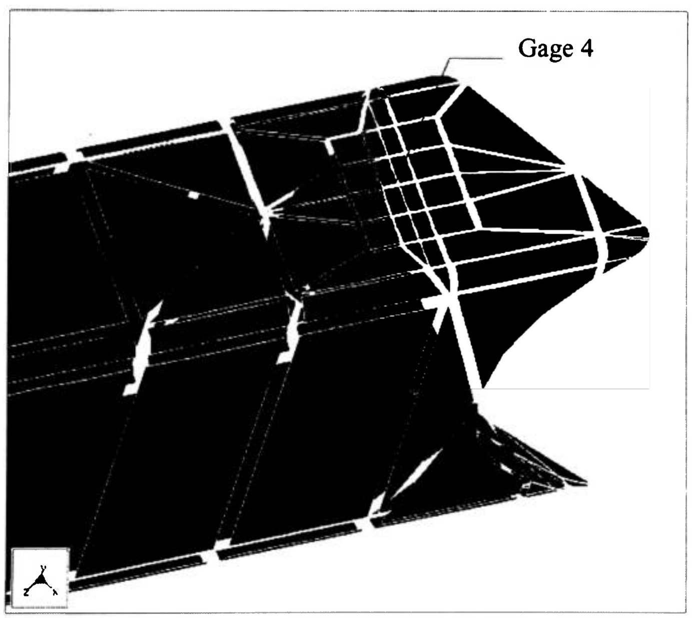

Figure 54. Gage 4 Remeshed Shell Elements, Run 2

Load	Exp. Strain	Run 1	% Diff.	Run 2	% Diff.
600 lbs.	-416.99	-511.7	-22.7%	-447.6	-7.3%
800 lbs.	-549.03	-692.5	-26.1%	-596.9	-8.7%
1000 lbs.	-681.07	-865.6	-27.1%	-746.1	-9.5%
1200 lbs.	-813.1	-1039	-27.8%	-895.3	-10.1%
1400 lbs.	-945.14	-1212	-28.2%	-1044	-10.5%

Table 6. Experimental vs Theoretical Strain, Gage 4

9.3 Gage R2

Gage R2, the rosette, demonstrated mixed results. The maximum principal strains improved, the minimum principal strains worsened. This location has very low strain levels in a multiple load region. It is conceivable that combining these two issues with the amount of welding in this area, some non-linear effects are occurring. Triangular elements were used for the mesh refinement only because they were easy to insert into the existing mesh for an initial attempt.

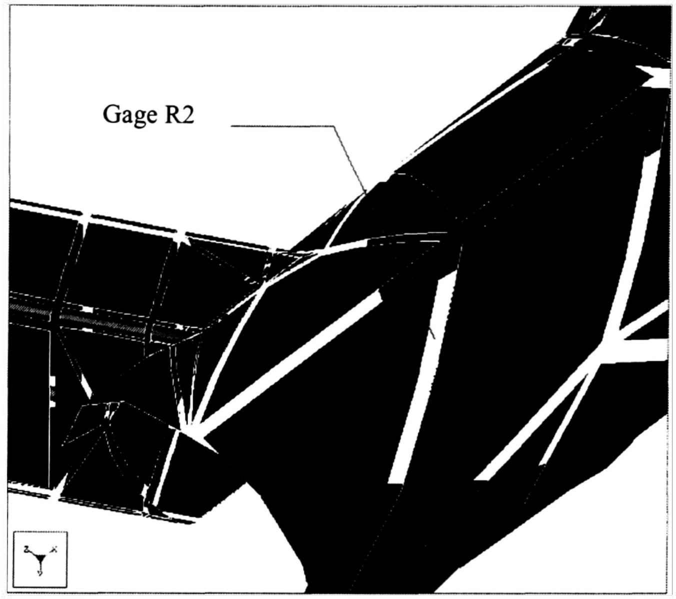

Figure 55. Gage R2 Shell Elements, Analysis Run 1

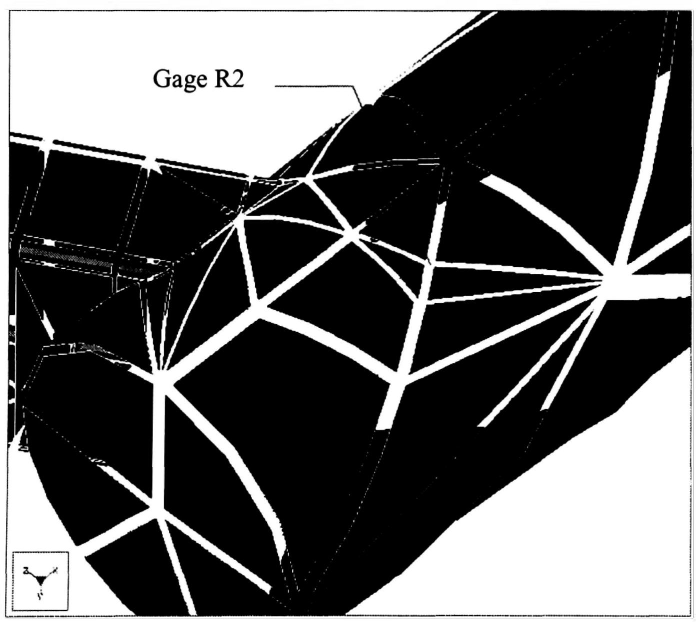

Figure 56. Gage R2 Remeshed Shell Elements, Analysis Run 2

Load	Exp. Strain	Run 1	% Diff.	Run 2	% Diff.
600 lbs.	88.34837	396.2001	-348.5%	206.0281	-133.2%
800 lbs.	129.4687	528.3001	-308.1%	274.5892	-112.1%
1000 lbs.	170.5908	660.3001	-287.1%	343.2652	-101.2%
1200 lbs.	211.7138	792.4001	-274.3%	411.9413	-94.6%
1400 lbs.	252.8372	924.5001	-265.7%	480.6072	-90.1%

Table 7. Experimental vs Theoretical Maximum Principal Strain, Gage R2

Load	Exp. Strain	Run 1	% Diff.	Run 2	% Diff.
600 lbs.	-484.293	-574.24	-18.6%	-46.3081	90.4%
800 lbs.	-644.156	-765.7	-18.9%	-61.7392	90.4%
1000 lbs.	-804.021	-957.1	-19.0%	-77.1752	90.4%
1200 lbs.	-963.887	-1148.5	-19.2%	-92.6113	90.4%
1400 lbs.	-1123.75	-1340	-19.2%	-108.037	90.4%

Table 8. Experimental vs Theoretical Minimum Principal Strain, Gage R2

10. Conclusions

In conclusion, do not believe everything a sales representative tells you. An FEA model which replicates the geometry of a structure does not guarantee accurate results. Determining loads and constraints is sometimes a formidable project itself. Combine this with the need to validate the analysis model with strain, load, acceleration, mode shape, or some experimentally derived or calculated physical parameter and the usefulness of analysis software packages becomes questionable. This is not an attempt to discredit finite element analysis as a useful engineering tool. The intent was to verify the manufacturer's claim that the software does not require correlation. That claim proved to be false. The uncertainties accompanying load and constraint sets will always require some level of correlation.

As a design tool, the Pro/Mechanica package is excellent. Numerous iterations can be performed quickly. Sensitivity studies are possible to determine which changes are most effective in reducing the overall stress, mass, cost, or many other user selectable parameters. The key is in the understanding that the final iteration may be far superior to the first, but the actual factor of safety is unknown until a correlation check is performed. Additionally, the accuracy of the safety factor will still be dependent on the accuracy of the loads and constraints used.

Provided accurate loads and constraints are available, the work completed here demonstrates a need for additional user generated mesh refinement in areas where accuracy is desired. The P Method does significantly reduce the number of elements required to analyze a part when compared to traditional FEA methods. The technique of using higher order equations to define complex states of deformation along large element edges not only reduces the number of elements, this in turn reduces computational time required for AutoGEM and the analysis engine.

Pro/Mechanica does have a point isolation setting with the AutoGEM feature. This technique places a small circle around geometry locations where two edges join with a 90 degree angle or less. While this does generate a ring of elements around geometry concentrations, it is still a blind technique. When this setting is toggled on, every location receives this ring of elements regardless of significance to the overall accuracy of the model. Overall, when compared to traditional H Methods, the Pro/Mechanica P Method is more efficient. Also, provisions have been made to allow the user to hand mesh and make up for the short comings of the AutoGEM routine.

The robustness of the AutoGEM routine is astounding. Even with the point isolation feature toggled on, the swingarm model never crashed during an AutoGEM sequence. Numerous shell and solid element models meshed by the author have also AutoGEM'd without even an error message. This is a significant improvement over the last two years. Even though hand meshing is required for improved accuracy, having the first 3000 elements generated automatically is an incredible time savings.

Unfortunately, the direction of the software as stated by Scott Kading, a PTC representative who spoke at the Mechanica Users Group, is to remove the meshing process from the user. Once the model has been defined geometrically, including loads and constraints, the software will mesh then run the analysis all in one step without the user ever seeing the mesh. Based on the work completed in this thesis project, the author believes that would be a serious setback to the accuracy of this software package. The AutoGEM routine is an excellent time saver for meshing 80%-90% of the model. The remaining 10%-20% should be redone by hand taking into consideration the required level of accuracy for all areas of concern.

Modeling stitch welds as elements may not be required depending on the proximity of surrounding geometry. For this particular project, both the single-sided and conventional swingarms are welded assemblies. It was thought that modeling the welds accurately would play a significant role in the overall accuracy. For the doubler plates, the results demonstrated the difference between simply increasing the material thickness versus modeling separate parts connected with elements in place of the stitch welds was insignificant. Presentations given at the Mechanica Users Group meetings have demonstrated that for other projects, weld modeling did play a role in the accuracy of the model. The author believes the minor effect displayed in this project is limited to the specific geometry involved. Perhaps if a major load path passed through the weld material, the effect of different modeling techniques would have been more pronounced.

When performing design cycles, it is acceptable to relax the convergence criteria to 20%-25%. This is important when using Pro/Mechanica as a design tool. Run times are drastically reduced by increasing the convergence criteria. Although test cases have been run by the author on the swingarm model, it is recommended that each model be checked independently.

The author's original intent for this project was to develop or learn effective modeling techniques. Checking results against experimental data was to be a one time step in the process. Once the techniques were validated, they could be used for other projects like the single-sided swingarm design. In retrospect, this was an optimistic if not foolish goal. The results demonstrate the need for some type of correlation check, whether it be strain, load, acceleration, mode shape, or some other experimentally measured parameter. If adequate correlation is not achieved, mesh refinement is probably necessary. Geometry changes to improve the accuracy of the modeled loads and constraints should be investigated as well.

The Pro/Mechanica FEA software is an excellent tool. While it does not perform at the level as described by the sales representatives, how many products are ever marketed conservatively? Used to assist in the design and development of new structures and systems it is a powerful tool. Used as the sole means of design for new structures and systems, it is simply dangerous.

BIBLIOGRAPHY

Beer, F. P., Johnston, E. R., Jr.(1981). Mechanics of Materials, New York: McGraw-Hill.

Buell Motorcycle Company, 2815 Buell Drive, East Troy, WI 53120. (414)-642-2020, www.Buell.com

HEM Data Corporation, 17336 West 12 Mile Road, Southfield, Michigan 48076-2123. (810) 559-5607

"Honda CBR900RR vs Kawasaki ZX-9R 900cc Street Fighters." Motorcycle Online Jul. 1986. www.motorcycle.com

IO Tech, Inc., 25971 Cannon Road, Cleveland, Ohio 44146. (216) 439-4091

King, R., Katsis, C., Balch, C. & Filip, D. (1991) Structural Analysis, Design, And Optimization With High-Order Finite Elements. (Available from Rasna Corporation, 701 Warrenville Road, Suite 350, Lisle, IL 60532)

Measurements Group, Inc., Micro-Measurements Division, PO Box 27777, Raleigh, NC 27611, USA. (919) 365-3800

Mechanica Users Group, Chicago/Milwaukee region. Bret Schaller, Chairman. (Information available from Parametric Technology Corporation, Waltham, MA.)

Miller, Scott. Director of Marketing, Buell Distribution Corporation. Program Development Meeting, 5 March 1996.

Motorcycle Online, 13441 Beach Avenue, Marina del Rey, CA 90292. On-line magazine located at www.motorcycle.com. CBR900 stoppie Tom Fortune. S2 sideshot courtesy of Buell Motorcycle Company.

Parametric Technology Corporation. Pro/Mechanica Design Study Reference. Waltham, MA 1995.

Parametric Technology Corporation. Pro/Mechanica Model Reference for Structure and Thermal. Waltham, MA 1995.

Peterson, Darryl. Application Engineer for Measurements Group, Inc., Micro-Measurements Division, PO Box 27777, Raleigh, NC 27611, USA. (919) 365-3800

Plane-Shear Measurement With Strain Gages. Tech Note 512. (Available from Measurements Group, Inc. PO Box 27777, Raleigh, NC 27611.

Rasna Corporation, 2590 North First St., #200, San Jose, CA 95131. (408) 922-6833, www.rasna.com

Sensotec, 1200 Chesapeake Avenue, Columbus, Ohio 43212. (614) 486-7723.

Smith, Carroll. (1978). Tune To Win, California: Aero Publishers, Inc.

Sporzynski, Steve, Rasna Engine Developer. (1995). 'Untitled'. Rasna Database Index: /Problem Solving/Engine/Applied Structure/Rel. 7.0.

Stein, Peter K. P.E. (1995). Verifying and Optimizing Transducer Accuracy, Seminar, Talladega Test Facility, AL. (Professor Stein teaches at Arizona State University)

Technimet Report #94347. Technimet Corporation. New Berlin, WI 53151.

Appendix A

Data Pt.	Gage 4	Load (lbs)
1	-84.0402	256.614
2	-89	263.5446
3	-92.031	267.821
4	-93.9598	265.6091
5	-90.9288	264.4294
6	-87.3468	264.4294
7	-87.0712	264.1345
8	-89.5511	263.2497
9	-89.5511	266.1989
10	-86.2446	262.8073
11	-85.418	265.904
12	-92.3065	265.0192
13	-90.3777	264.4294
14	-87.8978	263.1023
15	-87.3468	260.5955
16	-88.1734	264.7243
17	-90.9288	263.987
18	-90.6533	264.4294
19	-86.2446	261.7751
20	-88.7245	266.7887
21	-91.2044	260.1531
22	-90.3777	265.0192
23	-89.5511	262.5124
24	-85.6935	265.7565
25	-85.418	258.8259
26	-91.4799	263.8395
27	-90.1022	263.5446
28	-88.4489	262.9548
29	-86.2446	261.3327
30	-86.5201	263.5446
31	-90.6533	261.4802
32	-99.4706	262.365
33	-88.1734	265.3141
34	-87.6223	262.6599
35	-91.7554	265.6091
36	-93.4087	263.5446
37	-89.5511	265.7565
38	-88.7245	262.6599
39	-87.6223	270.0328
40	-95.062	267.9684
41	-94.7864	279.9126
42	-94.7864	291.267
43	-101.675	305.5706
44	-107.737	319.2843
45	-117.381	339.0438
46	-123.994	356.2966
47	-128.127	377.9731
48	-134.465	399.7971
49	-146.864	420.7363
50	-163.672	445.657
51	-160.641	462.4673
52	-159.815	484.8812
53	-168.081	503.6085
54	-175.796	518.9443
55	-175.245	516.8798
56	-175.796	518.5019
57	-172.214	515.1104
58	-172.49	516.8798
59	-178	514.8154
60	-176.623	516.8798
61	-171.938	516.8798
62	-173.316	512.1611
63	-180.205	514.5205
64	-176.623	513.9307
65	-176.898	516.7324
66	-172.49	513.4883
67	-176.623	516.1425
68	-176.623	512.3086
69	-175.796	516.4374
70	-174.969	511.1289
71	-176.898	514.5205
72	-171.112	512.751
73	-178.551	514.2256
74	-173.867	515.1104
75	-173.041	513.9307
76	-173.316	515.2578
77	-175.521	513.9307
78	-176.898	513.0459
79	-177.174	514.0781
80	-173.316	514.668
81	-172.214	512.0137
82	-176.898	516.29
83	-180.205	512.751
84	-171.663	512.6035
85	-172.214	511.4238
86	-170.561	514.0781
87	-177.174	518.3544
88	-179.378	525.7274
89	-182.685	538.7038
90	-192.604	553.0074

91	-191.502	569.6703
92	-203.901	585.1535
93	-209.688	603.291
94	-214.097	618.7743
95	-219.056	636.027
96	-227.874	654.4594
97	-242.753	673.6292
98	-243.029	692.0616
99	-250.744	715.6551
100	-259.561	739.8384
101	-271.134	760.1878
102	-278.849	782.0118
103	-284.084	794.1035
104	-282.431	798.6747
105	-284.084	801.4764
106	-287.942	802.5087
107	-286.289	798.8221
108	-284.635	801.9188
109	-282.707	799.1171
110	-281.88	808.1121
111	-275.818	796.7578
112	-283.533	800.0018
113	-284.635	799.412
114	-280.778	797.6425
115	-287.115	802.0663
116	-286.013	797.6425
117	-284.084	800.1493
118	-283.533	797.0527
119	-281.329	799.5594
120	-284.911	795.5781
121	-291.8	796.6103
122	-285.187	796.1679
123	-281.605	797.2001
124	-282.707	795.5781
125	-286.289	796.4628
126	-288.493	798.5272
127	-284.084	797.2001
128	-280.227	798.2323
129	-281.605	797.2001
130	-288.493	798.5272
131	-285.462	795.5781
132	-284.635	799.1171
133	-277.747	795.4306
134	-281.329	796.9052
135	-291.249	808.1121

136	-302.546	828.9039
137	-305.577	848.9583
138	-310.537	872.9942
139	-320.456	898.3572
140	-333.407	921.8033
141	-342.5	947.1663
142	-352.97	965.7462
143	-358.757	995.9753
144	-367.849	1017.504
145	-382.729	1041.835
146	-389.893	1066.019
147	-395.404	1088.727
148	-399.261	1106.127
149	-404.772	1113.943
150	-413.038	1112.616
151	-410.007	1109.519
152	-405.048	1109.372
153	-404.221	1110.404
154	-401.741	1109.961
155	-407.528	1108.044
156	-406.701	1110.109
157	-402.568	1103.768
158	-401.19	1108.929
159	-402.568	1107.012
160	-406.15	1107.455
161	-404.772	1104.948
162	-402.568	1105.538
163	-400.639	1108.634
164	-406.977	1106.127
165	-407.528	1107.602
166	-405.048	1104.358
167	-401.466	1107.75
168	-402.017	1105.538
169	-403.394	1107.16
170	-405.599	1103.326
171	-403.67	1106.717
172	-400.639	1105.98
173	-402.017	1105.39
174	-406.701	1104.063
175	-406.15	1104.8
176	-404.772	1106.717
177	-402.568	1104.358
178	-403.67	1105.98
179	-404.221	1103.621
180	-413.59	1105.833

181	-404.221	1104.358
182	-401.741	1105.39
183	-401.741	1101.999
184	-408.079	1106.717
185	-411.661	1120.431
186	-414.692	1139.748
187	-422.682	1161.867
188	-425.713	1173.369
189	-438.664	1187.083
190	-443.348	1205.22
191	-447.481	1221.883
192	-451.063	1238.399
193	-455.748	1257.716
194	-463.738	1273.641
195	-474.485	1301.511
196	-466.218	1312.128
197	-484.129	1333.215
198	-491.844	1353.859
199	-502.314	1372.882
200	-506.447	1390.577
201	-509.478	1399.277
202	-511.132	1405.028
203	-519.674	1409.009
204	-513.336	1409.599
205	-511.683	1405.028
206	-512.234	1407.534
207	-506.447	1403.701
208	-507.55	1405.175
209	-511.407	1403.111
210	-513.887	1406.207
211	-508.101	1404.29
212	-508.927	1403.996
213	-509.478	1404.29
214	-514.438	1401.489
215	-511.958	1402.226
216	-511.132	1402.226
217	-507.274	1402.963
218	-509.203	1401.931
219	-511.683	1401.931
220	-497.355	1401.784
221	-509.478	1401.341
222	-508.652	1397.802
223	-506.172	1400.456
224	-509.754	1397.95
225	-510.856	1399.719

226	-511.683	1397.065
227	-511.958	1399.129
228	-507.274	1398.097
229	-508.376	1398.687
230	-512.234	1397.802
231	-510.581	1398.097
232	-506.999	1397.212
233	-506.447	1391.904
234	-508.101	1398.245
235	-509.754	1397.95
236	-508.927	1392.789
237	-507.825	1401.636
238	-514.989	1417.562
239	-522.98	1444.989
240	-533.175	1461.947
241	-540.89	1486.573
242	-546.401	1505.742
243	-549.708	1533.17
244	-561.556	1555.289
245	-573.955	1584.781
246	-583.875	1605.572
247	-589.11	1633.442
248	-592.141	1651.285
249	-596.274	1670.602
250	-607.021	1681.219
251	-609.776	1694.785
252	-609.776	1698.324
253	-607.572	1698.619
254	-608.123	1699.209
255	-610.603	1695.228
256	-609.776	1694.933
257	-607.572	1691.984
258	-610.327	1693.901
259	-604.265	1692.278
260	-610.603	1692.721
261	-617.491	1690.214
262	-608.398	1692.131
263	-603.714	1689.624
264	-603.439	1691.394
265	-604.816	1688.74
266	-607.296	1691.836
267	-604.265	1688.592
268	-604.816	1696.112
269	-605.092	1689.477
270	-609.501	1688.887

271	-609.501	1689.329
272	-607.021	1687.412
273	-603.163	1689.772
274	-602.336	1684.758
275	-608.949	1683.726
276	-608.674	1686.233
277	-605.918	1688.445
278	-602.061	1685.348
279	-603.99	1688.002
280	-602.061	1685.643
281	-608.123	1686.675
282	-605.918	1682.399
283	-604.541	1685.79
284	-609.776	1683.431
285	-602.061	1685.2
286	-607.021	1686.528
287	-606.47	1680.629
288	-604.541	1686.085
289	-602.336	1681.956
290	-605.092	1689.624
291	-612.531	1698.767
292	-616.114	1719.559
293	-621.349	1732.977
294	-627.962	1753.769
295	-630.442	1769.4
296	-643.392	1791.666
297	-648.077	1812.753
298	-656.067	1837.231
299	-670.395	1860.972
300	-669.844	1884.271
301	-680.866	1909.634
302	-686.928	1932.342
303	-689.408	1957.116
304	-696.021	1976.433
305	-689.132	1993.833
306	-699.328	1989.114
307	-703.736	1990.884
308	-704.287	1986.755
309	-699.328	1985.428
310	-699.879	1981.004
311	-698.501	1983.806
312	-704.012	1981.151
313	-701.256	1979.972
314	-700.154	1978.645
315	-694.919	1979.972
316	-704.563	1979.087
317	-700.705	1977.907
318	-697.95	1976.285
319	-696.848	1977.907
320	-694.919	1976.433
321	-704.838	1976.728
322	-698.776	1976.728
323	-699.052	1975.548
324	-696.572	1973.484
325	-695.745	1975.253
326	-693.266	1973.926
327	-695.194	1974.073
328	-696.848	1975.253
329	-694.092	1973.778
330	-700.154	1978.202
331	-697.95	1972.009
332	-693.541	1974.368
333	-698.776	1971.714
334	-699.328	1973.778
335	-690.51	1971.272
336	-693.541	1972.304
337	-692.163	1969.355
338	-697.399	1971.567
339	-697.399	1969.945
340	-695.194	1970.239
341	-693.266	1972.009
342	-691.888	1970.829
343	-691.888	1966.848
344	-695.745	1968.322
345	-696.021	1970.829
346	-695.194	1971.714
347	-692.99	1972.009
348	-692.714	1972.894
349	-701.256	1985.428
350	-706.767	2000.174
351	-708.145	2018.164
352	-713.38	2029.96
353	-718.064	2053.407
354	-725.78	2070.217
355	-734.597	2094.105
356	-740.383	2121.533
357	-746.17	2137.458
358	-750.854	2160.609
359	-759.396	2183.171
360	-770.693	2202.93

361	-774	2222.837
362	-779.786	2244.072
363	-785.021	2258.228
364	-785.021	2260.882
365	-786.95	2260.292
366	-787.501	2260.44
367	-791.634	2254.836
368	-784.47	2258.08
369	-779.51	2254.541
370	-780.062	2254.983
371	-783.919	2254.099
372	-780.888	2256.163
373	-781.99	2252.182
374	-778.408	2252.182
375	-781.164	2250.412
376	-783.368	2254.099
377	-783.644	2248.938
378	-783.093	2250.855
379	-782.817	2249.233
380	-779.235	2248.938
381	-778.133	2248.938
382	-782.817	2247.463
383	-785.297	2251.297
384	-780.062	2245.694
385	-778.133	2246.283
386	-777.857	2247.316
387	-783.368	2249.38
388	-782.541	2247.906
389	-780.613	2247.168
390	-779.786	2245.989
391	-776.204	2246.578
392	-778.684	2243.777
393	-782.817	2252.919
394	-780.337	2245.251
395	-778.959	2245.694
396	-785.572	2242.892
397	-777.857	2245.251
398	-779.235	2239.5
399	-780.337	2242.892
400	-779.235	2240.68
401	-777.031	2242.155
402	-776.755	2239.205
403	-775.653	2242.892
404	-781.164	2241.27
405	-781.99	2242.744

406	-777.031	2242.892
407	-776.479	2242.007
408	-776.479	2243.629
409	-777.306	2249.233
410	-785.021	2263.536
411	-798.247	2275.48
412	-796.319	2294.355
413	-788.328	2311.166
414	-803.207	2332.252
415	-816.158	2352.012
416	-826.077	2374.131
417	-826.904	2392.71
418	-829.659	2416.599
419	-836.823	2435.031
420	-843.436	2459.067
421	-849.498	2479.859
422	-855.836	2497.407
423	-860.244	2510.236
424	-858.04	2515.102
425	-856.938	2512.448
426	-858.316	2512.005
427	-860.796	2511.858
428	-860.796	2510.088
429	-856.387	2509.203
430	-856.387	2506.254
431	-856.938	2507.581
432	-861.347	2506.549
433	-861.071	2507.434
434	-866.031	2503.158
435	-859.693	2503.452
436	-858.04	2504.337
437	-853.632	2506.107
438	-858.867	2501.978
439	-855.836	2503.158
440	-856.662	2500.651
441	-852.529	2502.273
442	-852.529	2499.914
443	-857.214	2500.061
444	-861.347	2499.766
445	-855.285	2501.536
446	-855.56	2499.029
447	-854.183	2497.702
448	-857.765	2497.554
449	-856.938	2495.342
450	-855.009	2495.785

451	-855.285	2497.849
452	-853.08	2497.112
453	-850.325	2497.112
454	-852.805	2495.785
455	-860.796	2495.637
456	-855.285	2494.605
457	-855.009	2489.886
458	-851.152	2495.195
459	-840.957	2494.752
460	-852.805	2493.573
461	-855.009	2490.771
462	-854.734	2491.951
463	-855.56	2489.739
464	-848.396	2491.213
465	-851.427	2479.564
466	-853.356	2487.822
467	-852.529	2483.988
468	-849.774	2484.135
469	-848.396	2483.103
470	-848.672	2484.283
471	-846.743	2481.923
472	-853.356	2482.956
473	-852.805	2482.808
474	-858.316	2484.578
475	-848.947	2484.283
476	-851.703	2483.988
477	-857.214	2499.619
478	-863	2521.148
479	-868.235	2543.856
480	-875.124	2566.123
481	-880.635	2590.011
482	-886.421	2612.867
483	-895.79	2638.083
484	-905.158	2659.022
485	-913.424	2681.731
486	-915.353	2699.721
487	-917.006	2712.255
488	-915.078	2720.218
489	-923.619	2722.725
490	-921.966	2718.596
491	-920.037	2719.923
492	-918.935	2715.204
493	-913.7	2716.974
494	-913.975	2713.14
495	-920.588	2716.384

496	-915.904	2711.96
497	-916.455	2713.14
498	-916.731	2716.384
499	-922.793	2711.518
500	-913.149	2709.306
501	-920.037	2706.799
502	-917.282	2708.864
503	-920.864	2709.158
504	-914.802	2708.421
505	-914.802	2708.126
506	-914.802	2709.748
507	-916.18	2707.831
508	-916.18	2709.453
509	-915.904	2707.979
510	-915.904	2705.177
511	-912.322	2706.504
512	-917.833	2708.126
513	-915.078	2705.03
514	-916.18	2706.652
515	-914.251	2705.325
516	-911.495	2705.472
517	-913.149	2704.735
518	-905.709	2706.357
519	-915.078	2703.408
520	-916.731	2704.587
521	-913.149	2702.228
522	-924.722	2703.555
523	-912.598	2700.163
524	-917.006	2702.67
525	-926.099	2698.689
526	-912.873	2700.016
527	-910.118	2698.394
528	-918.109	2698.689
529	-909.016	2697.067
530	-912.873	2696.624
531	-916.731	2692.79
532	-912.873	2692.79
533	-912.598	2691.021
534	-914.251	2690.726
535	-907.362	2688.956
536	-912.322	2691.021
537	-921.415	2690.578
538	-907.913	2688.219
539	-908.189	2691.463
540	-915.353	2690.578

541	-907.087	2691.758
542	-913.975	2689.399
543	-911.771	2690.136
544	-914.251	2688.367
545	-908.189	2691.168
546	-904.882	2689.546
547	-909.016	2691.906
548	-911.495	2690.873
549	-910.393	2695.297
550	-913.7	2699.279
551	-915.353	2714.319
552	-919.211	2726.706
553	-922.517	2740.567
554	-931.059	2749.71
555	-937.672	2765.635
556	-936.019	2777.58
557	-937.397	2794.832
558	-943.183	2818.426
559	-954.48	2829.338
560	-956.409	2839.955
561	-961.093	2858.092
562	-965.226	2871.806
563	-967.431	2888.027
564	-970.462	2898.791
565	-980.932	2912.063
566	-981.483	2920.468
567	-980.381	2925.776
568	-978.177	2921.057
569	-976.524	2919.878
570	-974.319	2922.385
571	-973.217	2918.403
572	-975.146	2916.929
573	-979.279	2921.942
574	-978.728	2916.929
575	-974.044	2914.569
576	-973.493	2915.159
577	-973.493	2910.44
578	-976.799	2916.044
579	-976.799	2911.03
580	-976.524	2914.274
581	-974.044	2911.178
582	-973.768	2911.915
583	-970.737	2908.966
584	-975.146	2911.03
585	-975.421	2908.376

586	-972.115	2910.883
587	-974.595	2906.901
588	-970.462	2908.671
589	-972.666	2906.017
590	-967.706	2911.62
591	-973.768	2904.984
592	-971.839	2906.164
593	-973.493	2908.376
594	-972.39	2905.279
595	-968.257	2903.362
596	-969.635	2904.247
597	-973.493	2898.644
598	-968.808	2904.247
599	-972.115	2899.233
600	-969.359	2903.215
601	-971.013	2903.362
602	-969.911	2901.445
603	-972.666	2899.233
604	-972.39	2898.349
605	-969.084	2897.464
606	-968.257	2893.04
607	-964.675	2893.335
608	-965.226	2887.142
609	-971.288	2888.322
610	-966.88	2890.533
611	-970.186	2888.911
612	-966.329	2886.257
613	-965.502	2890.091
614	-964.4	2888.027
615	-960.267	2891.271
616	-968.808	2890.681
617	-974.044	2900.413
618	-973.217	2908.376
619	-976.524	2924.596
620	-982.31	2942.292
621	-987.27	2960.724
622	-996.363	2973.7
623	-997.74	2991.248
624	-1002.98	3007.469
625	-1006.83	3020.74
626	-1016.75	3038.877
627	-1014	3054.803
628	-1021.44	3069.107
629	-1024.47	3082.525
630	-1027.5	3092.258

631	-1030.53	3103.612
632	-1032.73	3108.478
633	-1028.33	3112.902
634	-1029.15	3108.331
635	-1033.29	3108.773
636	-1032.73	3107.446
637	-1031.08	3106.414
638	-1026.12	3104.644
639	-1026.4	3103.76
640	-1024.47	3104.792
641	-1031.91	3100.811
642	-1031.08	3101.843
643	-1027.22	3100.811
644	-1023.92	3100.516
645	-1029.43	3097.714
646	-1025.85	3105.087
647	-1034.94	3093.88
648	-1029.98	3099.336
649	-1029.15	3094.912
650	-1027.22	3096.829
651	-1014.27	3094.175
652	-1027.77	3094.027
653	-1023.37	3093.88
654	-1027.77	3095.355
655	-1026.95	3090.341
656	-1024.74	3093.585
657	-1022.81	3090.193
658	-1021.99	3093.88
659	-1022.54	3090.341
660	-1025.85	3090.636
661	-1027.77	3089.309
662	-1027.5	3090.931
663	-1024.19	3086.802
664	-1021.44	3088.866
665	-1023.09	3087.392
666	-1024.19	3088.571
667	-1026.12	3086.949
668	-1025.57	3085.917
669	-1023.64	3084.59
670	-1021.99	3086.212
671	-1020.33	3084.148
672	-1021.16	3084.442
673	-1025.29	3081.198
674	-1024.47	3083.853
675	-1021.99	3082.231

676	-1021.99	3082.083
677	-1021.44	3080.756
678	-1021.71	3082.083
679	-1018.96	3081.051
680	-1023.09	3079.576
681	-1024.19	3082.083
682	-1025.29	3080.314
683	-1019.23	3080.314
684	-1019.78	3077.07
685	-1018.41	3076.922
686	-1017.58	3075.742
687	-1021.99	3075.153
688	-1018.68	3071.614
689	-1014	3072.941
690	-1015.1	3069.992
691	-1006.01	3071.024
692	-1015.65	3066.158
693	-1020.61	3065.863
694	-1018.41	3063.798
695	-1017.86	3064.978
696	-1020.89	3060.554
697	-1017.58	3063.798
698	-1014	3057.605
699	-1017.3	3059.227
700	-1015.93	3054.066
701	-1013.45	3055.688
702	-1012.9	3052.444
703	-1010.97	3052.444
704	-1009.59	3050.527
705	-1003.8	3049.495
706	-1013.17	3046.545
707	-1013.72	3047.873
708	-1011.24	3044.923
709	-1019.23	3045.071
710	-1008.76	3040.647
711	-1008.49	3039.762
712	-1008.21	3037.403
713	-1009.04	3037.845
714	-1008.76	3033.569
715	-1008.21	3035.928
716	-1006.83	3032.094
717	-1004.9	3032.684
718	-1008.76	3028.703
719	-1010.69	3029.883
720	-1007.66	3027.818

721	-1006.28	3024.869
722	-1003.53	3024.574
723	-1001.87	3024.869
724	-1002.15	3023.099
725	-1002.42	3021.33
726	-1005.46	3022.657
727	-1004.35	3018.971
728	-1004.35	3024.869
729	-1004.9	3015.431
730	-1000.77	3016.611
731	-999.669	3012.187
732	-996.363	3009.386
733	-1008.76	3010.123
734	-1001.05	3009.975
735	-999.118	3001.865
736	-996.914	3016.316
737	-1000.5	3005.847
738	-996.363	3005.404
739	-996.363	3003.045
740	-999.669	3004.815
741	-1010.42	3000.096
742	-997.74	2999.064
743	-994.709	2997.884
744	-994.158	2997.884
745	-994.158	2994.197
746	-993.332	2994.345
747	-996.363	2991.248
748	-998.291	2992.428
749	-993.332	2990.658
750	-991.403	2989.626
751	-985.617	2985.94
752	-993.056	2989.331
753	-994.709	2984.318
754	-992.505	2984.318
755	-991.127	2983.138
756	-989.75	2983.433
757	-990.025	2980.041
758	-988.096	2980.926
759	-989.474	2978.272
760	-993.056	2978.862
761	-990.576	2974.88
762	-992.781	2977.092
763	-988.096	2971.931
764	-986.994	2975.028
765	-985.617	2969.277

766	-987.545	2972.963
767	-988.923	2967.655
768	-988.372	2967.36
769	-988.096	2967.065
770	-989.474	2966.622
771	-989.199	2962.494
772	-984.239	2964.263
773	-982.31	2959.102
774	-992.23	2959.397
775	-985.341	2957.038
776	-983.412	2955.71
777	-984.239	2952.466
778	-981.208	2955.268
779	-979.003	2951.139
780	-979.83	2950.254
781	-982.861	2949.37
782	-980.381	2948.19
783	-979.003	2945.241
784	-978.452	2944.503
785	-977.626	2945.388
786	-976.799	2944.061
787	-979.555	2942.144
788	-980.381	2938.9
789	-979.003	2939.048
790	-978.452	2936.393
791	-979.555	2937.278
792	-974.595	2934.034
793	-982.861	2933.297
794	-973.217	2927.841
795	-980.381	2930.495
796	-975.146	2926.956
797	-974.595	2925.776
798	-973.493	2924.891
799	-969.635	2925.776
800	-971.013	2921.057
801	-967.431	2922.827
802	-974.044	2918.993
803	-974.044	2918.403
804	-971.013	2913.98
805	-969.635	2917.076
806	-967.431	2912.652
807	-967.982	2913.685
808	-966.329	2910.293
809	-969.084	2911.325
810	-967.431	2907.196

811	-963.849	2909.113
812	-969.911	2904.542
813	-963.849	2903.067
814	-963.573	2902.92
815	-963.573	2898.644
816	-971.839	2899.233
817	-967.982	2898.496
818	-964.951	2895.989
819	-963.849	2895.989
820	-966.053	2893.188
821	-961.369	2894.662
822	-961.093	2890.386
823	-971.288	2888.911
824	-964.675	2888.027
825	-960.267	2886.257
826	-961.093	2884.783
827	-957.787	2884.635
828	-960.542	2881.538
829	-955.031	2882.423
830	-949.52	2881.096
831	-959.716	2879.179
832	-959.44	2879.769
833	-956.684	2876.82
834	-956.96	2877.409
835	-955.031	2874.903
836	-958.062	2875.05
837	-962.746	2874.608
838	-959.44	2872.691
839	-956.409	2868.267
840	-956.684	2869.889
841	-943.183	2865.023
842	-950.898	2868.857
843	-958.889	2865.465
844	-949.52	2865.318
845	-952.827	2861.042
846	-953.102	2862.221
847	-952.276	2858.977
848	-950.898	2856.765
849	-943.458	2856.175
850	-956.133	2857.06
851	-947.041	2854.111
852	-953.378	2853.963
853	-950.623	2851.162
854	-948.143	2849.54
855	-947.592	2848.95

856	-946.489	2850.277
857	-943.183	2846.296
858	-948.143	2847.328
859	-945.663	2844.526
860	-947.316	2844.821
861	-946.214	2841.429
862	-945.938	2842.904
863	-942.632	2837.596
864	-939.325	2838.628
865	-940.703	2836.268
866	-943.183	2834.499
867	-945.938	2832.287
868	-943.734	2834.204
869	-942.907	2832.877
870	-943.458	2831.845
871	-939.876	2832.287
872	-935.743	2828.748
873	-936.019	2829.633
874	-942.081	2834.794
875	-943.183	2828.453
876	-941.805	2825.356
877	-939.325	2824.914
878	-937.121	2822.997
879	-936.845	2823.44
880	-934.09	2821.965
881	-939.601	2821.67
882	-939.601	2817.836
883	-936.294	2818.426
884	-937.672	2815.624
885	-934.917	2817.099
886	-933.263	2811.348
887	-933.539	2814.592
888	-935.192	2810.463
889	-940.703	2811.643
890	-938.223	2810.021
891	-933.263	2811.348
892	-932.712	2805.744
893	-930.783	2806.481
894	-930.232	2805.744
895	-929.406	2806.334
896	-934.641	2801.468
897	-932.161	2802.058
898	-929.13	2800.731
899	-930.232	2798.371
900	-928.579	2796.307

901	-928.028	2796.897
902	-927.752	2794.39
903	-931.335	2795.717
904	-928.028	2793.063
905	-928.579	2793.948
906	-927.201	2794.537
907	-934.917	2790.556
908	-923.895	2790.998
909	-923.344	2787.902
910	-926.099	2788.344
911	-927.477	2785.247
912	-929.13	2784.363
913	-926.099	2780.529
914	-923.068	2780.234
915	-922.793	2779.644
916	-921.966	2779.939
917	-918.935	2778.612
918	-922.517	2778.022
919	-924.446	2774.041
920	-922.793	2775.663
921	-920.037	2773.008
922	-919.762	2773.156
923	-918.66	2770.944
924	-918.935	2768.585
925	-910.944	2768.29
926	-920.588	2768.437
927	-926.926	2765.93
928	-918.66	2766.225
929	-917.833	2765.045
930	-915.078	2760.917
931	-915.353	2760.327
932	-918.384	2763.128
933	-918.384	2754.134
934	-918.935	2760.179
935	-916.455	2752.954
936	-913.424	2758.557
937	-912.598	2751.774
938	-917.833	2754.134
939	-915.629	2752.659
940	-915.629	2751.774
941	-915.078	2749.562
942	-913.7	2749.415
943	-914.251	2747.055
944	-910.669	2746.466
945	-910.393	2745.286

946	-910.669	2745.728
947	-914.802	2742.779
948	-913.975	2743.516
949	-899.372	2742.042
950	-915.353	2739.388
951	-905.709	2737.765
952	-906.811	2736.586
953	-904.882	2739.093
954	-905.709	2737.176
955	-909.842	2736.438
956	-911.22	2735.406
957	-910.669	2734.816
958	-897.994	2731.13
959	-905.158	2731.277
960	-904.607	2727.886
961	-902.127	2723.167
962	-908.465	2727.296
963	-908.465	2726.264
964	-902.954	2723.462
965	-904.331	2721.398
966	-900.749	2721.545
967	-902.403	2723.315
968	-902.678	2716.826
969	-904.607	2720.955
970	-906.26	2717.564
971	-903.505	2719.333
972	-901.576	2716.089
973	-901.3	2717.269
974	-899.923	2714.909
975	-899.096	2714.467
976	-898.821	2708.716
977	-813.127	2444.764
978	-651.934	1886.63
979	-422.407	1249.311
980	-223.741	702.2363
981	-105.257	342.7303
982	-45.7398	171.53
983	-19.8388	90.7222
984	-16.8078	49.876
985	-13.5013	36.4572
986	-11.0214	24.0706
987	-9.9192	20.5316
988	-7.4393	14.6332
989	-6.0616	17.4349
990	-6.0616	11.0942

991	-10.1948	12.4213
992	-9.0926	6.3755
993	-10.7458	6.9653
994	-3.0306	-3.9467
995	-2.7551	1.6568
996	-1.3774	-1.7348
997	-1.3774	3.2788
998	0.5514	1.5093
999	-2.7551	3.2788
1000	-3.5817	-1.8822
1001	-13.5013	1.6568
1002	-4.1328	1.8042
1003	0.827	2.8365
1004	0.827	0.6246
1005	0.0003	2.0992
1006	-5.7861	-0.2602
1007	-5.235	1.0669
1008	-3.3062	-1.4399
1009	-4.6839	-0.5551
1010	0.2759	-0.85
1011	0.0003	1.2144
1012	2.7558	-0.85
1013	0.5514	2.5415
1014	-4.1328	-0.85
1015	-5.235	1.0669
1016	-2.7551	0.772
1017	-4.9594	0.9195
1018	-1.1018	-0.85
1019	0.2759	1.3619
1020	-0.8263	0.3297
1021	-4.6839	3.1314
1022	-3.0306	-1.7348
1023	-4.1328	-1.8822
1024	4.6846	0.0347
1025	-0.5508	2.689
1026	1.6536	0.1822
1027	0.2759	1.3619
1028	-4.6839	-0.7026
1029	-3.0306	0.772
1030	-2.204	0.1822
1031	-0.8263	-1.5873
1032	-1.9285	-0.2602
1033	0.827	1.6568
1034	-5.7861	-1.5873
1035	-3.8573	0.3297

1036	-4.6839	0.4771
1037	-11.848	2.8365
1038	-1.6529	-1.4399
1039	0.2759	-0.1127
1040	-2.204	-0.7026
1041	-0.8263	0.9195
1042	1.1025	0.0347
1043	0.827	0.772
1044	-1.3774	-0.4076
1045	-2.7551	1.5093
1046	-0.2752	-3.0619
1047	-1.6529	1.0669
1048	2.2047	-1.5873
1049	1.6536	-0.4076
1050	0.2759	-0.1127
1051	-4.9594	0.4771
1052	-2.204	-1.7348
1053	-4.1328	1.2144
1054	-0.5508	-0.2602
1055	-1.3774	1.0669
1056	1.9291	-1.1449
1057	0.2759	0.4771
1058	0.827	-3.9467
1059	-4.1328	0.9195
1060	-1.3774	-0.7026
1061	-1.9285	-0.4076
1062	-1.6529	-1.4399
1063	-0.5508	-0.7026
1064	0.827	-1.2924
1065	1.6536	-0.1127
1066	-4.1328	-1.2924
1067	-4.1328	-1.7348
1068	-3.5817	-0.7026
1069	-5.7861	0.1822
1070	-0.8263	0.0347
1071	0.2759	0.1822
1072	0.827	-3.3568
1073	1.1025	0.9195
1074	-2.4796	-0.4076
1075	-0.8263	0.3297
1076	-4.1328	-0.9975
1077	-3.0306	0.772
1078	-0.8263	-2.6195
1079	1.1025	0.4771
1080	-0.2752	-1.4399

1081	-3.3062	2.689
1082	-4.1328	-1.2924
1083	-2.4796	0.0347
1084	-0.5508	-2.0297
1085	-0.2752	-2.0297
1086	3.0313	-1.7348
1087	-0.2752	-1.1449
1088	4.6846	-1.7348
1089	-3.3062	-2.6195
1090	-1.3774	-1.5873
1091	-0.5508	-1.5873
1092	-1.6529	-1.4399
1093	0.5514	-0.1127
1094	0.5514	2.8365
1095	-1.6529	-0.2602
1096	-3.0306	-5.2738
1097	-2.4796	-0.85
1098	-2.7551	-2.767
1099	-2.4796	0.6246
1100	-3.3062	-2.3246
1101	1.378	-0.4076
1102	5.5112	-1.5873
1103	3.3068	-2.4721
1104	-3.5817	-1.5873
1105	-11.848	2.2466
1106	-9.6437	-1.7348
1107	-3.8573	-0.2602
1108	0.5514	-1.5873
1109	1.378	-0.1127
1110	1.378	-1.7348
1111	2.7558	-0.5551
1112	-5.7861	-3.0619
1113	-4.1328	0.6246
1114	-4.6839	-1.7348
1115	-3.0306	0.3297
1116	2.2047	-2.4721
1117	0.0003	-0.2602
1118	0.827	-4.0941
1119	-3.8573	-0.1127
1120	-2.204	-0.7026
1121	-4.1328	7.5552
1122	-1.1018	-0.2602
1123	-1.6529	-0.1127
1124	1.1025	-0.4076
1125	1.378	0.0347

1126	-2.204	-3.9467
1127	-4.4084	-1.8822
1128	-2.4796	0.6246
1129	-3.0306	0.1822
1130	-0.2752	-0.5551
1131	0.5514	-2.4721
1132	-4.1328	1.5093
1133	1.378	-1.2924
1134	-3.0306	0.3297
1135	-1.3774	-0.7026
1136	-0.8263	-0.1127
1137	1.6536	-1.5873
1138	-3.8573	-0.7026
1139	-2.7551	-1.7348
1140	2.7558	1.3619
1141	-12.1236	-1.1449
1142	-1.6529	0.3297
1143	-2.7551	-1.4399
1144	-1.3774	4.606
1145	-0.5508	-1.1449
1146	2.2047	-2.4721
1147	2.2047	-0.7026
1148	0.0003	-1.2924
1149	-2.204	-0.7026
1150	-4.1328	1.3619
1151	-1.6529	-0.2602
1152	-0.2752	-0.2602
1153	0.5514	-0.4076
1154	0.5514	0.772
1155	0.827	-1.1449
1156	-3.0306	-0.9975
1157	-3.5817	-2.1772
1158	-2.204	1.3619
1159	-3.8573	-1.5873
1160	-0.2752	-0.2602
1161	-5.7861	-2.1772
1162	4.1335	-0.85
1163	2.2047	-0.7026
1164	11.2976	0.4771
1165	-2.204	-1.2924
1166	3.0313	-3.0619
1167	-2.4796	0.1822
1168	1.6536	0.9195
1169	0.827	-0.1127
1170	2.7558	0.3297

1171	-3.3062	-0.7026
1172	-3.0306	0.1822
1173	-5.5105	-0.9975
1174	-1.6529	-3.0619
1175	0.0003	-1.5873
1176	0.2759	1.0669
1177	2.2047	-1.8822
1178	-7.9904	0.4771
1179	-1.1018	-0.9975
1180	-0.2752	1.5093
1181	-1.9285	0.0347
1182	-4.1328	-0.2602
1183	1.378	-2.6195
1184	1.1025	0.4771
1185	-0.5508	-3.2094
1186	-4.1328	1.5093
1187	5.7867	-1.7348
1188	-3.0306	0.1822
1189	-0.2752	-2.6195
1190	0.827	6.3755
1191	1.6536	-1.2924
1192	3.5824	-0.4076
1193	-9.6437	-3.6518
1194	0.5514	-0.4076
1195	-1.3774	-1.8822
1196	-4.1328	0.9195
1197	1.378	-6.306
1198	-0.5508	1.2144
1199	1.1025	-2.4721
1200	0.827	-0.1127
1201	-4.1328	-2.4721
1202	-1.3774	-0.9975
1203	-4.1328	-3.0619
1204	-1.3774	-2.9145
1205	1.378	-2.0297
1206	4.9601	-0.2602
1207	1.6536	-3.6518
1208	-2.204	-1.1449
1209	-3.0306	-4.389
1210	-2.7551	-1.7348
1211	-0.2752	-1.7348
1212	2.4802	-0.1127
1213	1.1025	-3.6518
1214	0.2759	-0.7026
1215	5.2356	-0.4076

1216	-2.204	-0.2602
1217	-0.5508	-0.9975
1218	-2.7551	-4.684
1219	-3.0306	-0.7026
1220	1.6536	1.2144
1221	1.6536	-3.5043
1222	0.2759	0.772
1223	-3.5817	-1.2924
1224	-7.1638	-0.4076
1225	-2.4796	-3.0619
1226	0.5514	-0.5551
1227	1.1025	-1.7348
1228	3.5824	1.6568
1229	-4.1328	-1.2924
1230	0.0003	0.4771
1231	-0.8263	-2.0297
1232	-1.9285	-3.0619
1233	-1.3774	-0.4076
1234	0.5514	0.1822
1235	1.378	-3.3568
1236	1.1025	-1.1449
1237	0.2759	-2.1772
1238	-2.7551	-1.4399
1239	-2.4796	-2.3246
1240	-6.8882	-1.1449
1241	0.2759	-5.1263
1242	0.0003	-1.5873
1243	1.1025	-9.1077
1244	1.378	-0.9975
1245	-1.3774	-3.9467
1246	-2.7551	-7.6332
1247	-1.6529	-3.6518
1248	-0.2752	-0.1127
1249	4.1335	-3.0619
1250	-7.7149	-1.2924
1251	1.9291	-2.4721
1252	-0.8263	-0.9975
1253	-1.3774	-4.2416
1254	0.5514	-1.5873
1255	-2.204	-3.0619
1256	-2.7551	-1.4399
1257	12.9508	-3.7992
1258	1.9291	-0.85
1259	0.2759	-3.7992
1260	-2.204	-7.6332

1261	-1.6529	-2.0297
1262	-0.5508	-5.7162
1263	0.5514	-1.7348
1264	1.1025	-1.5873
1265	1.9291	-0.4076
1266	2.2047	-0.2602
1267	-1.9285	-1.4399
1268	1.378	-2.1772
1269	-1.3774	-1.5873
1270	-1.6529	-2.3246
1271	1.1025	1.3619
1272	15.9818	-2.1772
1273	2.4802	0.4771
1274	-3.3062	-1.7348
1275	-1.6529	-0.5551
1276	-1.3774	-2.0297
1277	14.6041	-1.2924
1278	0.827	-3.0619
1279	1.9291	-5.1263
1280	1.378	-3.7992
1281	2.7558	-1.1449
1282	-3.0306	-2.767
1283	-1.3774	-1.4399
1284	-0.2752	-3.6518
1285	-1.3774	-4.2416
1286	1.9291	-2.0297
1287	2.7558	-3.6518
1288	-4.9594	-2.6195
1289	-2.4796	-1.2924
1290	-3.0306	-2.3246
1291	-3.3062	-2.0297
1292	1.1025	-2.1772
1293	1.1025	0.4771
1294	1.1025	-1.8822
1295	1.378	5.0484
1296	2.7558	-1.8822
1297	-3.0306	0.1822
1298	-3.3062	-3.0619
1299	0.0003	-1.7348
1300	1.378	-6.0111
1301	1.378	0.4771
1302	2.2047	-2.767
1303	1.6536	0.6246
1304	-3.5817	-3.6518
1305	-2.7551	-0.7026

1306	-1.6529	-3.7992
1307	0.5514	-0.1127
1308	4.1335	-3.0619
1309	1.9291	-0.1127
1310	1.6536	-1.2924
1311	-2.7551	-3.5043
1312	-3.0306	-2.0297
1313	-3.3062	-0.5551
1314	1.6536	-3.3568
1315	2.7558	-3.3568
1316	2.2047	-1.5873
1317	0.2759	-1.1449
1318	-0.2752	-2.9145
1319	-1.9285	-4.0941
1320	-0.5508	-3.2094
1321	2.4802	-1.5873
1322	0.0003	-3.9467
1323	-0.2752	-1.4399
1324	-0.8263	-2.1772
1325	2.7558	-2.9145
1326	-1.9285	-4.2416
1327	1.378	-2.767
1328	-11.0214	-3.6518
1329	0.2759	-2.0297
1330	-3.8573	-2.767
1331	1.378	-2.9145
1332	-3.8573	-2.9145
1333	-1.1018	-2.0297
1334	-1.3774	-0.85
1335	-1.9285	-2.6195
1336	-1.9285	-4.9789
1337	0.0003	-2.0297
1338	2.4802	-1.2924
1339	0.0003	-2.3246
1340	0.0003	-0.7026
1341	0.0003	-3.3568
1342	-0.8263	-0.85
1343	-0.5508	-2.6195
1344	0.827	-3.0619
1345	2.2047	-3.2094
1346	0.5514	-1.4399
1347	3.0313	-3.3568
1348	-1.9285	0.9195
1349	-1.9285	-2.0297
1350	-2.7551	-4.389

1351	-1.1018	-1.7348
1352	-0.8263	-0.9975
1353	1.9291	-2.0297
1354	3.3068	0.3297
1355	-2.4796	-3.0619
1356	-1.6529	2.2466
1357	-1.6529	-1.7348
1358	8.2666	0.1822
1359	1.6536	-2.4721
1360	-0.8263	0.4771
1361	1.378	-6.4535
1362	0.827	-2.4721
1363	-2.204	-3.5043
1364	0.5514	-0.1127
1365	0.5514	-3.7992
1366	1.9291	0.3297
1367	1.9291	-5.7162
1368	1.378	-0.85
1369	1.1025	-2.9145
1370	-1.9285	-2.3246
1371	-0.8263	-4.0941
1372	0.0003	-2.0297
1373	-1.3774	-2.6195
1374	2.7558	-1.5873
1375	2.7558	-3.0619
1376	2.7558	-1.2924
1377	-4.6839	-2.9145
1378	-1.3774	-1.8822
1379	-1.3774	1.0669
1380	0.5514	-0.1127
1381	-0.2752	-2.4721
1382	1.378	-2.3246
1383	-4.4084	-4.389
1384	-1.3774	-2.0297
1385	0.0003	-2.1772
1386	-1.3774	-1.5873
1387	-1.6529	-1.8822
1388	1.378	-2.4721
1389	2.7558	-0.9975
1390	4.409	-1.2924
1391	3.8579	0.1822
1392	-2.204	-2.767
1393	-9.0926	-0.4076
1394	0.0003	-2.4721
1395	-0.5508	-0.4076

1396	3.0313	-2.767
1397	1.378	-0.85
1398	-0.2752	-2.9145
1399	-2.204	-3.6518
1400	-2.204	-0.7026
1401	-1.6529	-4.5365
1402	-1.1018	-3.6518
1403	1.1025	0.4771
1404	3.3068	-2.6195
1405	2.2047	5.4907
1406	-1.9285	-2.767
1407	0.2759	-0.9975
1408	0.2759	-3.2094
1409	2.7558	-1.5873
1410	-3.8573	-5.4213
1411	-6.0616	-1.5873
1412	-15.9812	-0.85
1413	-4.1328	-0.85
1414	-6.6127	-3.0619
1415	-4.4084	-1.2924
1416	-3.3062	-3.0619
1417	12.3998	-1.8822
1418	0.2759	-3.0619
1419	3.3068	-2.767
1420	2.2047	-4.0941
1421	-3.0306	-0.9975
1422	14.6041	-2.767
1423	1.6536	-2.1772
1424	2.2047	-4.5365
1425	3.0313	-1.5873
1426	2.4802	-5.4213
1427	-2.7551	1.3619
1428	-1.9285	-4.2416
1429	-6.0616	-2.3246
1430	-6.6127	-4.684
1431	-12.9502	-0.9975
1432	-2.7551	-2.4721
1433	-9.3681	-1.5873
1434	1.6536	-4.2416
1435	0.5514	-2.6195
1436	-1.1018	-3.7992
1437	-1.3774	-2.1772
1438	9.6443	-2.4721
1439	2.2047	-1.5873
1440	2.2047	-2.6195

1441	1.378	-0.2602
1442	1.378	-2.0297
1443	-0.8263	-7.7806
1444	-1.9285	-0.2602
1445	-1.1018	-1.1449
1446	-0.2752	-1.5873
1447	0.0003	-3.0619
1448	1.6536	-0.9975
1449	1.378	-2.4721
1450	-3.8573	-0.85
1451	-2.7551	-1.7348
1452	-1.3774	-0.1127
1453	1.6536	-2.9145
1454	3.8579	-1.2924
1455	3.5824	-3.0619
1456	-7.4393	-2.0297
1457	-2.4796	-2.4721
1458	-1.3774	0.6246
1459	0.2759	-2.1772
1460	-4.9594	0.3297
1461	1.378	-3.9467
1462	1.9291	-2.0297
1463	2.2047	-1.2924
1464	-1.1018	-1.8822
1465	-2.204	-2.6195
1466	-5.7861	-0.9975
1467	-2.204	-3.3568
1468	0.2759	-0.4076
1469	5.2356	-2.0297
1470	2.7558	-0.9975
1471	3.3068	-2.6195
1472	-1.6529	0.9195
1473	-4.1328	-0.9975
1474	0.0003	0.1822
1475	-0.2752	-2.3246
1476	0.5514	2.8365
1477	0.5514	-1.2924
1478	0.827	-0.2602
1479	-3.5817	-2.3246
1480	1.378	0.0347
1481	-0.2752	-1.8822
1482	-6.0616	-0.7026
1483	0.827	-7.6332
1484	1.1025	-1.1449
1485	4.9601	-3.3568

1486	0.0003	-0.7026
1487	-6.0616	-2.1772
1488	-1.3774	-0.2602
1489	-1.3774	-2.6195
1490	-1.9285	-1.7348
1491	2.2047	-0.9975
1492	-3.3062	-0.7026
1493	0.2759	-7.1908
1494	-3.5817	-2.4721
1495	-1.9285	-1.8822
1496	-0.8263	-2.1772
1497	-2.7551	-0.1127
1498	2.2047	-6.6009
1499	1.378	0.6246
1500	2.7558	-3.0619